

Diffuse Emission Models Confront the Galactic Center Excess

Tim Linden

CCAPP Postdoctoral Fellow

Center for Cosmology and Astro-Particle Physics

The Ohio State University

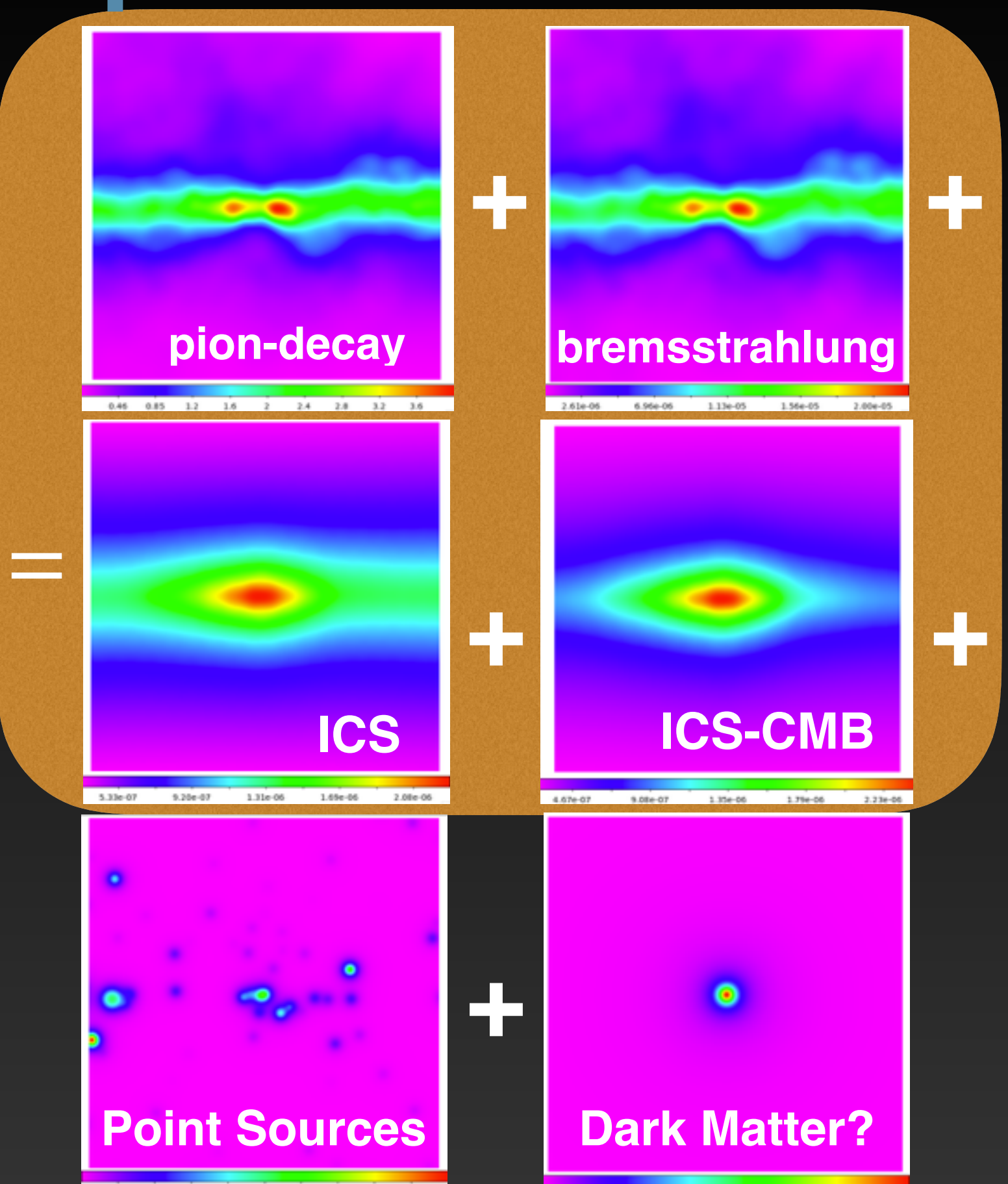
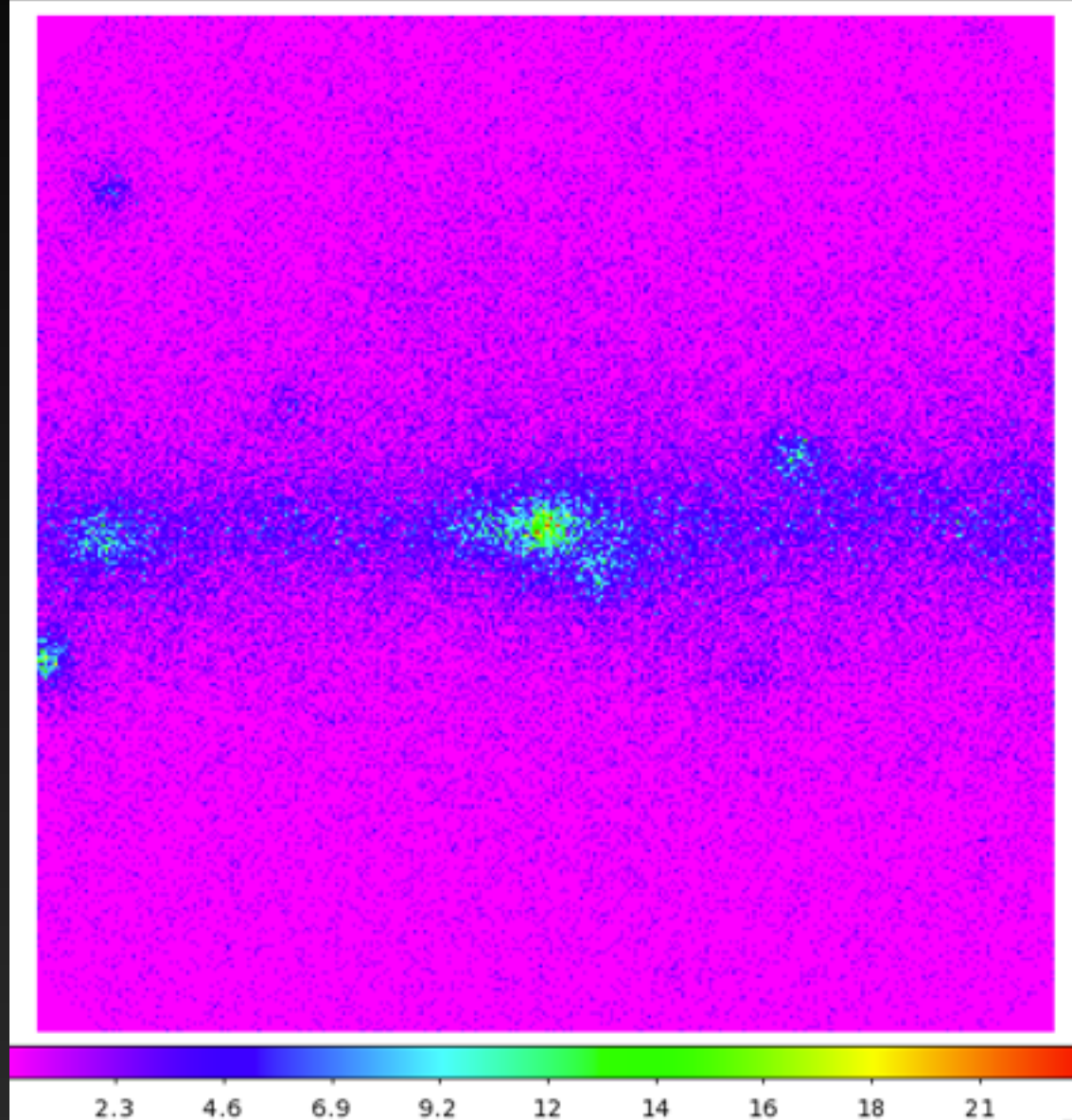


THE OHIO STATE
UNIVERSITY

2016 CETUP Workshop

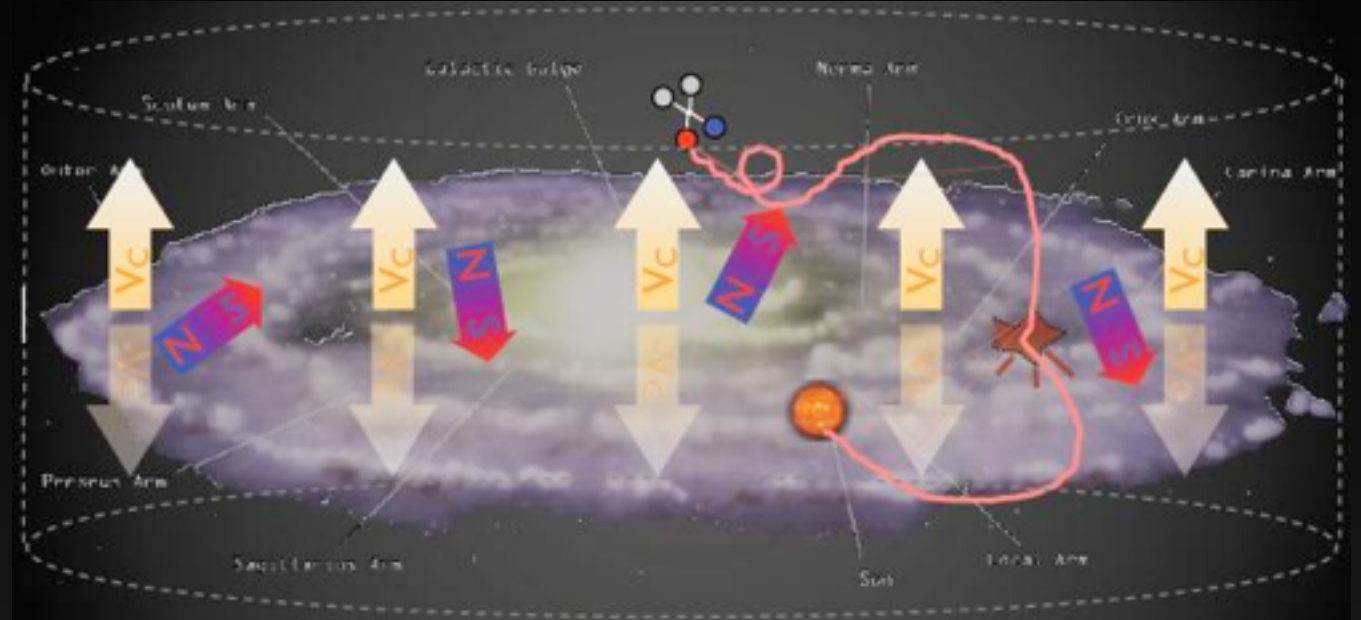
7/7/16

Untangling the spider's web



Diffuse Emission Modeling

Models of diffuse gamma-ray emission depend sensitively on the Galactic cosmic-ray distribution.



Cosmic-Rays are thought to be accelerated primarily by supernovae events, and then take $\sim 10^8 — 10^9$ years to escape the Milky Way magnetic field.

What we need is a catalog of all Galactic supernovae over the past billion years.

Observations of the historical supernova rate can fail in two ways:

- 1.) Observational incompleteness
- 2.) Time variability

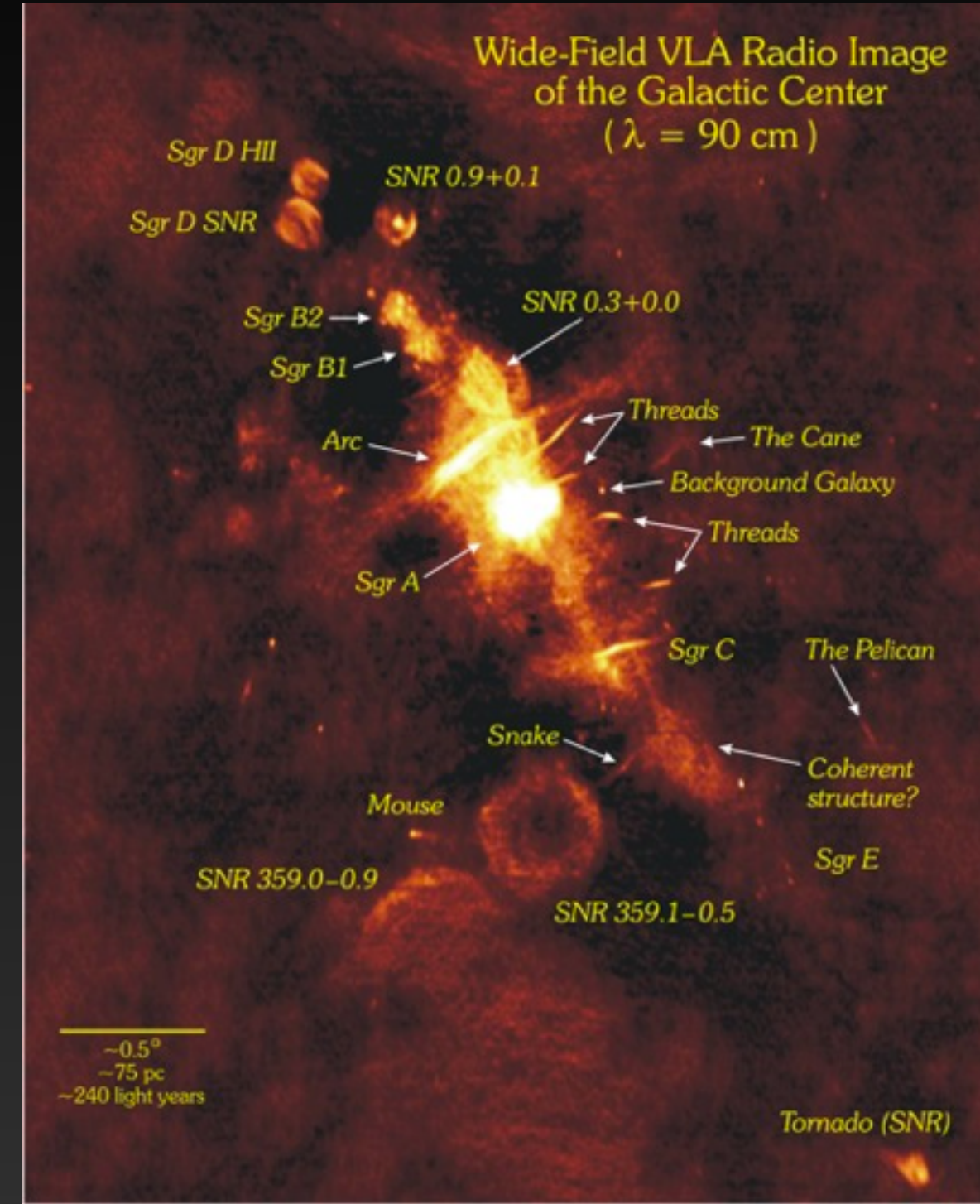
The Problem



Chandra

Multiwavelength observations indicate that the Galactic Center is a dense star-forming environment.

3-20% of the total Galactic Star Formation Rate is contained within the Central Molecular Zone.



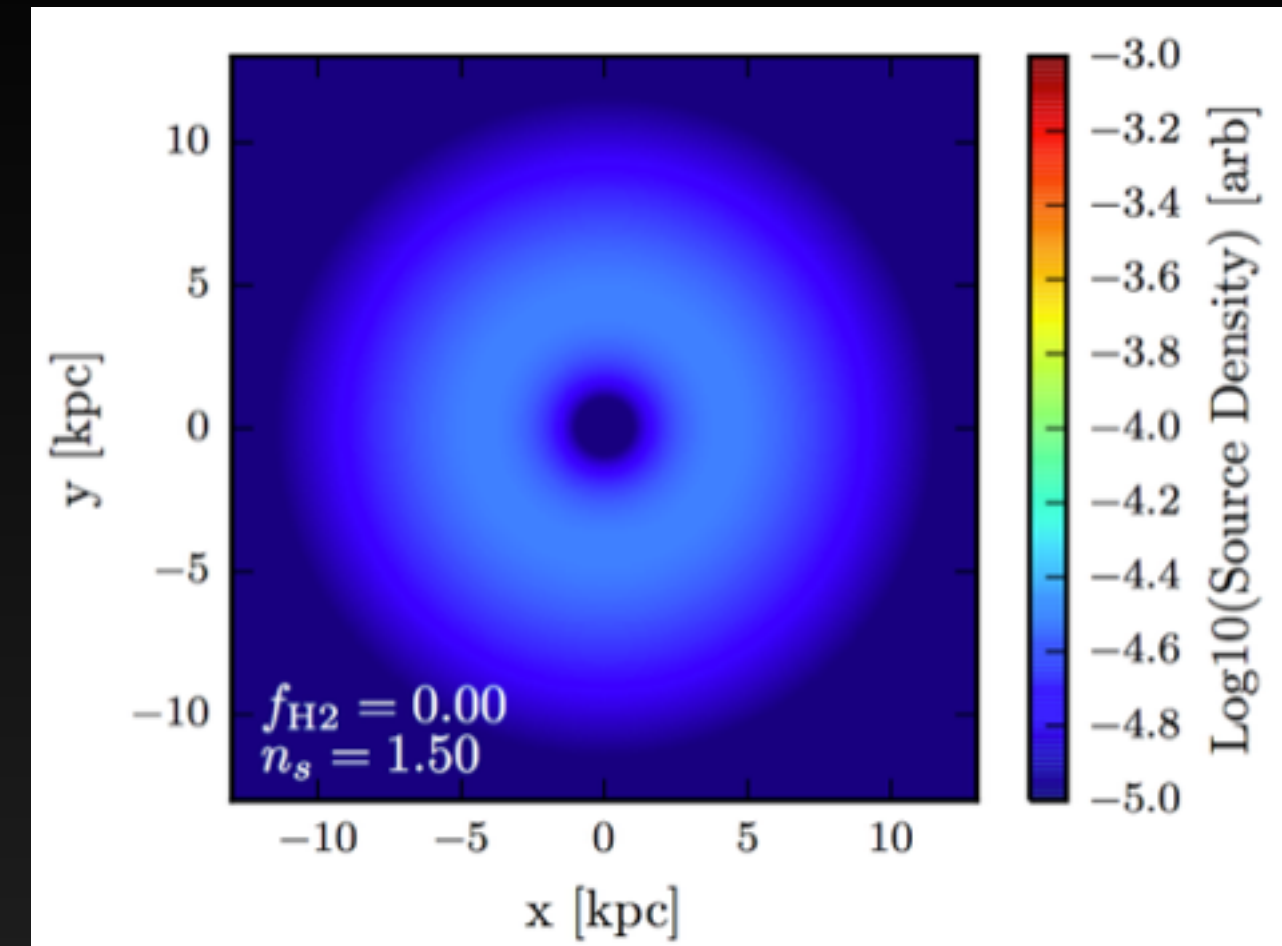
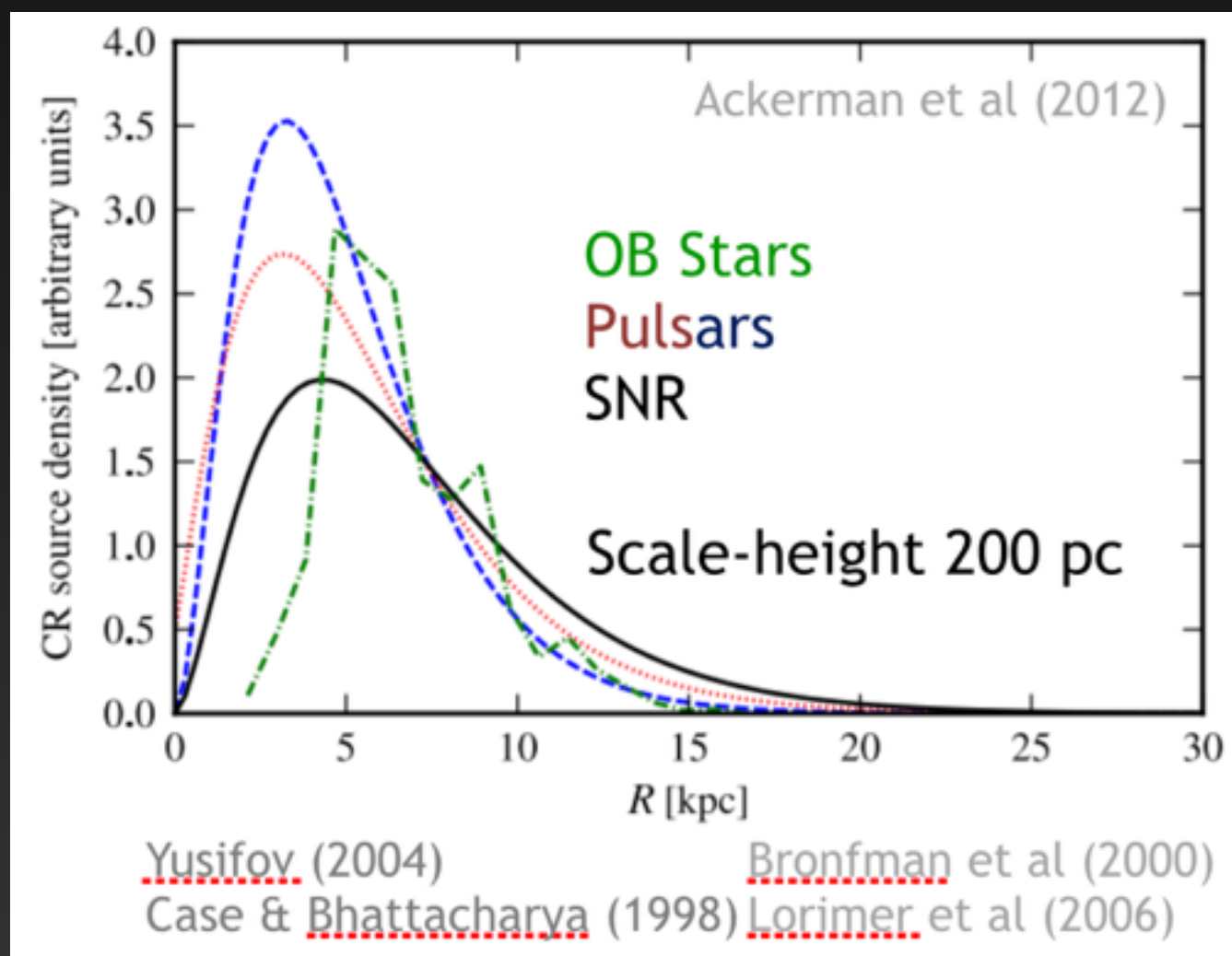
The Problem

Measurements of Star Formation Rate:

- 1.) 2-4% - ISOGL Survey Immer et al. (2012)
- 2.) 2.5-5% - Young Stellar Objects Yusef-Zadeh et al. (2009)
- 3.) 5-10% - Infrared Flux Longmore et al. (2013)
- 4.) 10-20% - Wolf-Rayet Stars Rosslowe & Crowther (2014)
- 5.) 2% - Far-IR Flux Thompson et al. (2007)
- 6.) 2.5-6% - SN1a Schanne et al. (2007)

The Problem

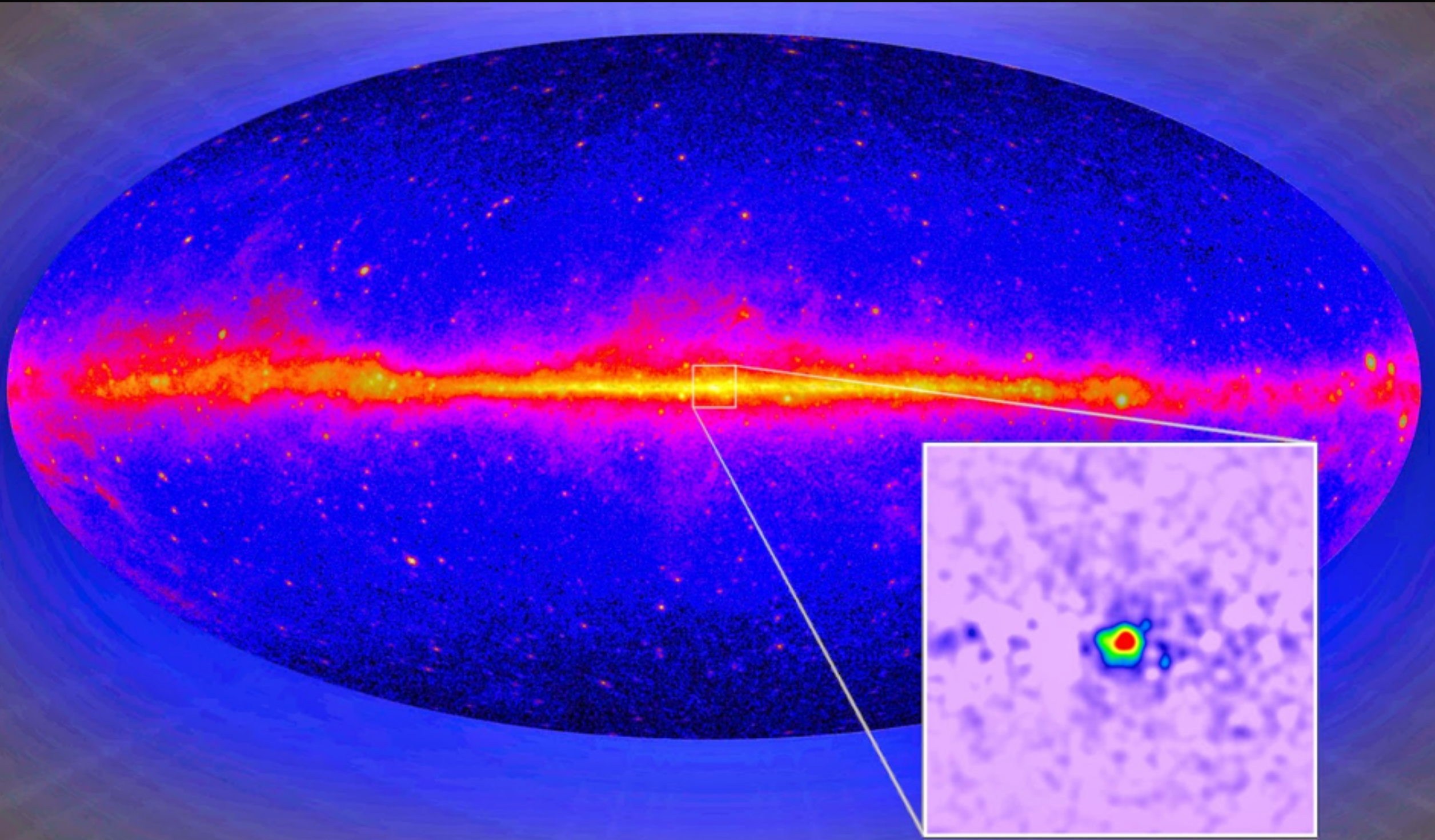
Cosmic-Ray Propagation Codes (e.g. Galprop), generally utilize a cosmic-ray injection rate at the Galactic center that is identically 0.



Results from these cosmic-ray propagation codes are used in many analyses of the Galactic center region.

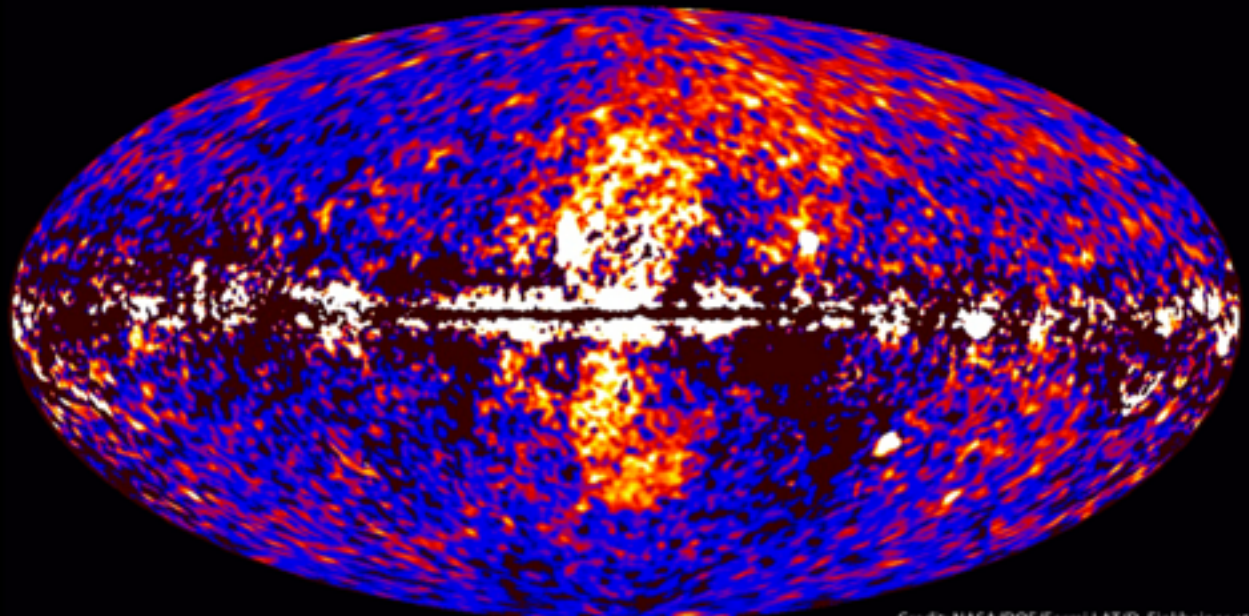
Carlson et al. (2016a, 2016b)
1510.04698
1603.06584

Fool me once, shame on, shame on you...

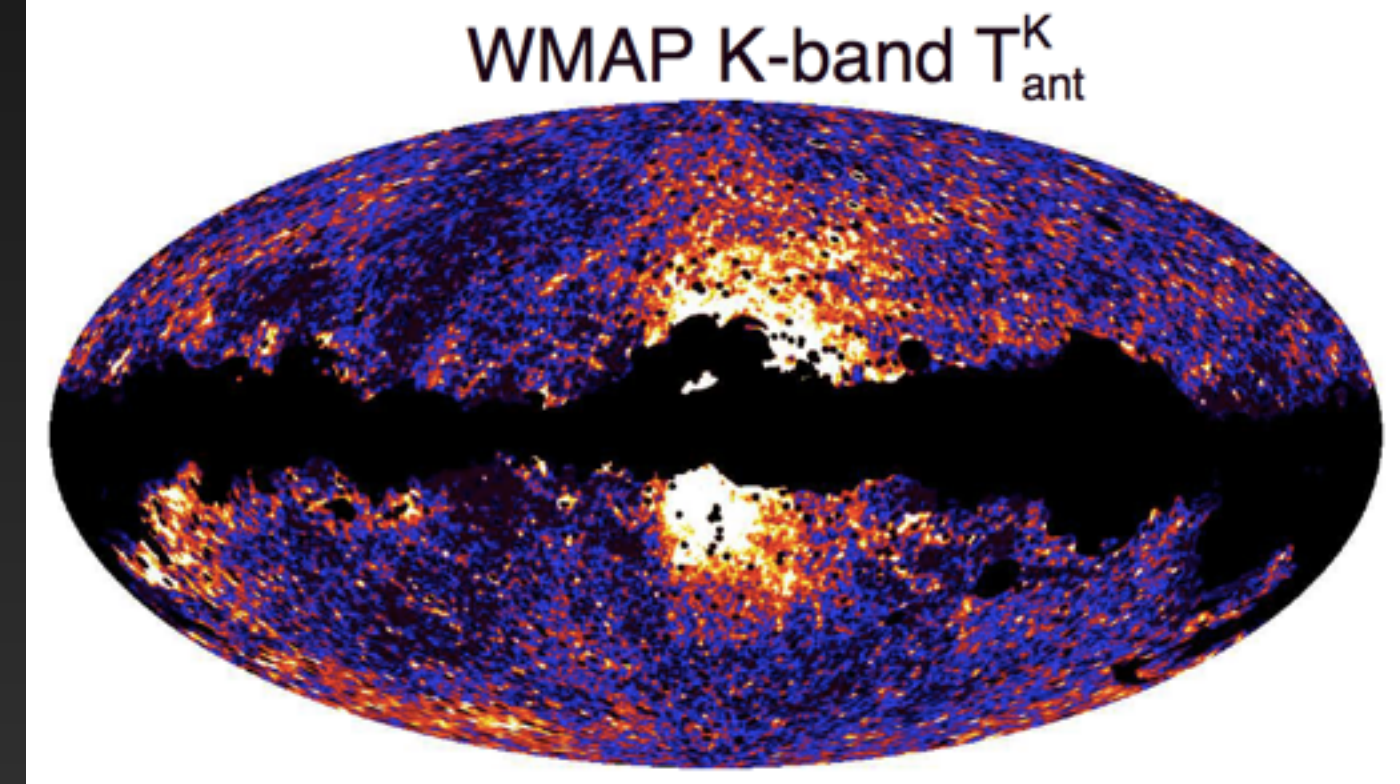
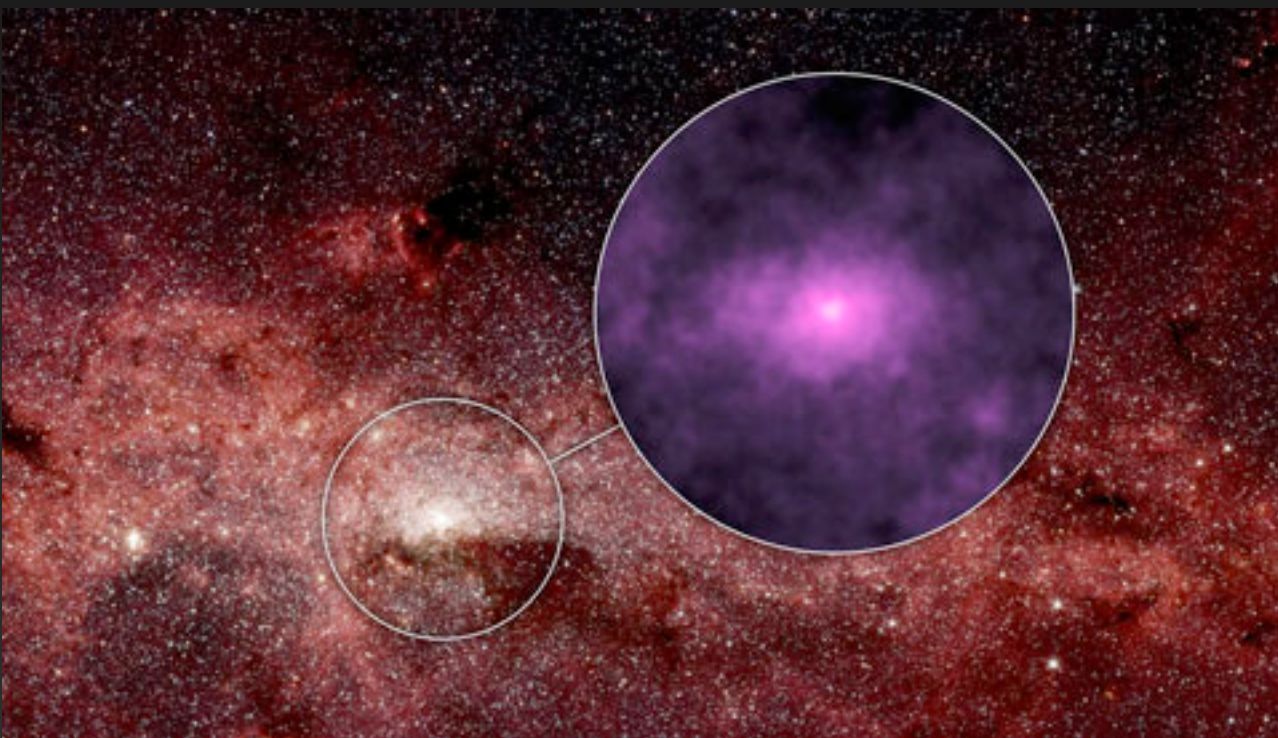
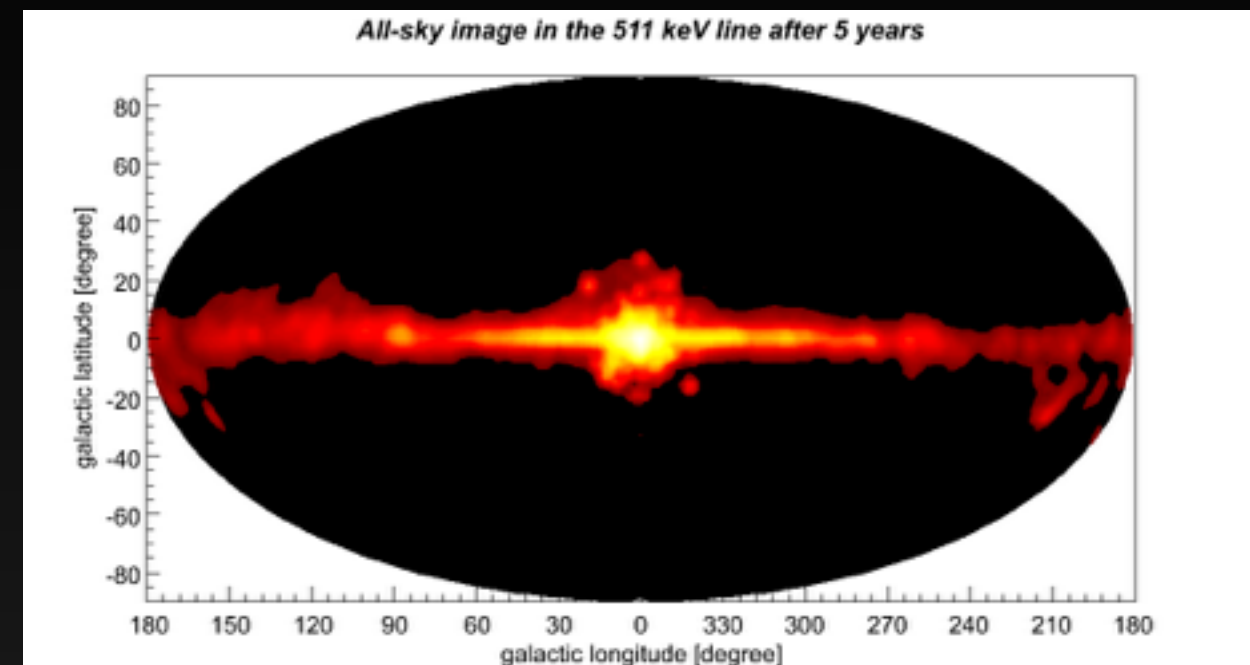


Fool me — you can't get fooled again!

Fermi data reveal giant gamma-ray bubbles



Credit: NASA/DOE/Fermi LAT/D. Finkbeiner et al.

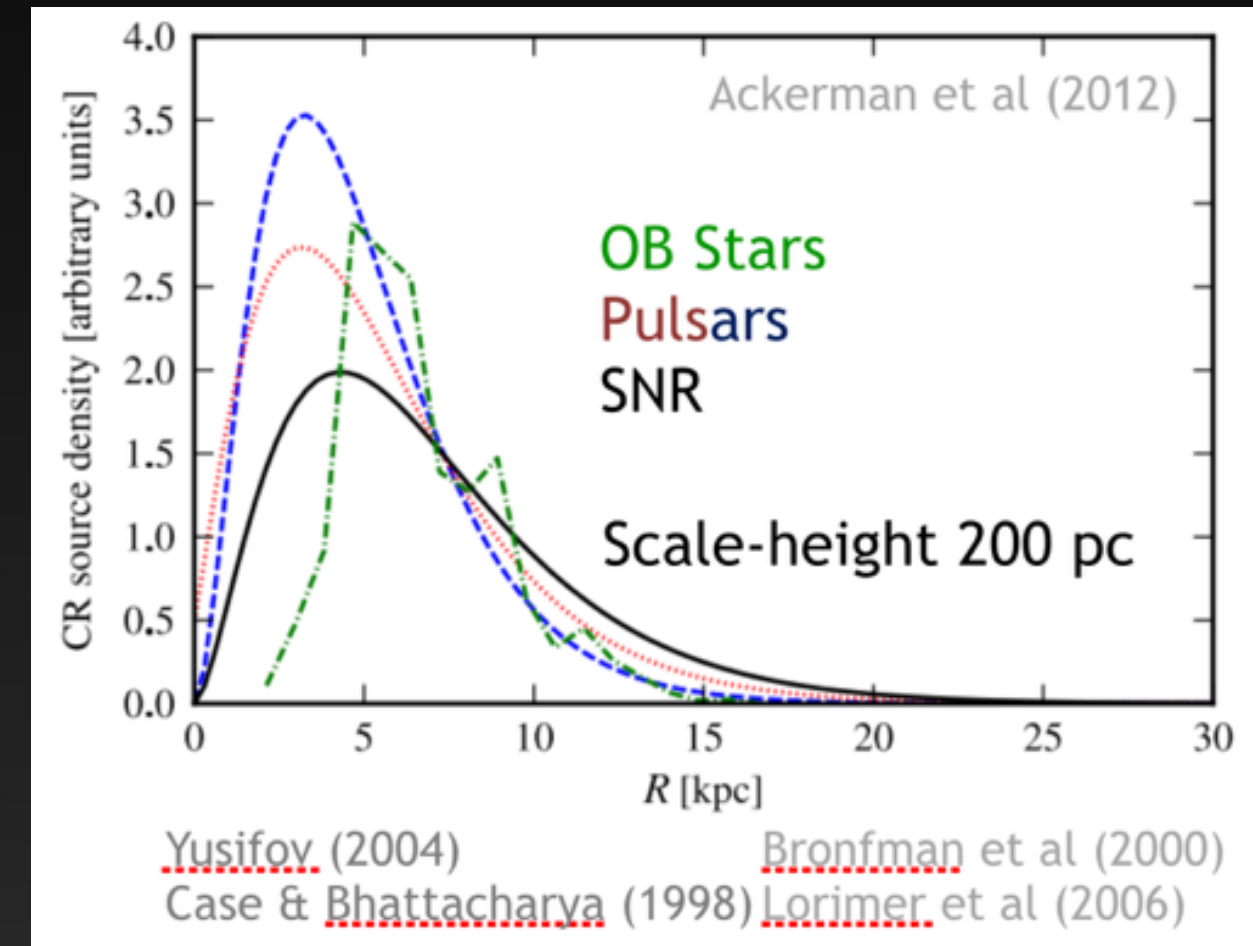


What we've got here is a failure to communicate

1.) The Galactic Center star formation rate is based on targeted observations. However, cosmic-ray diffusion models need a equal sensitivity throughout the Galaxy:

- + Observed SNR
- + Pulsars
- + OB Stars

2.) The Galactic center cosmic-ray injection rate does not significantly affect the observed primary-to-secondary cosmic-ray population at Earth.



3.) Computational models (Galprop) are significantly faster if the cosmic-ray injection rate is fit to a simple analytic form.

The Solution

Solution: Add a new cosmic-ray injection morphology tracing the molecular gas density.

Observationally Resilient: Several tracers of molecular gas are sensitive to the galactic center region.

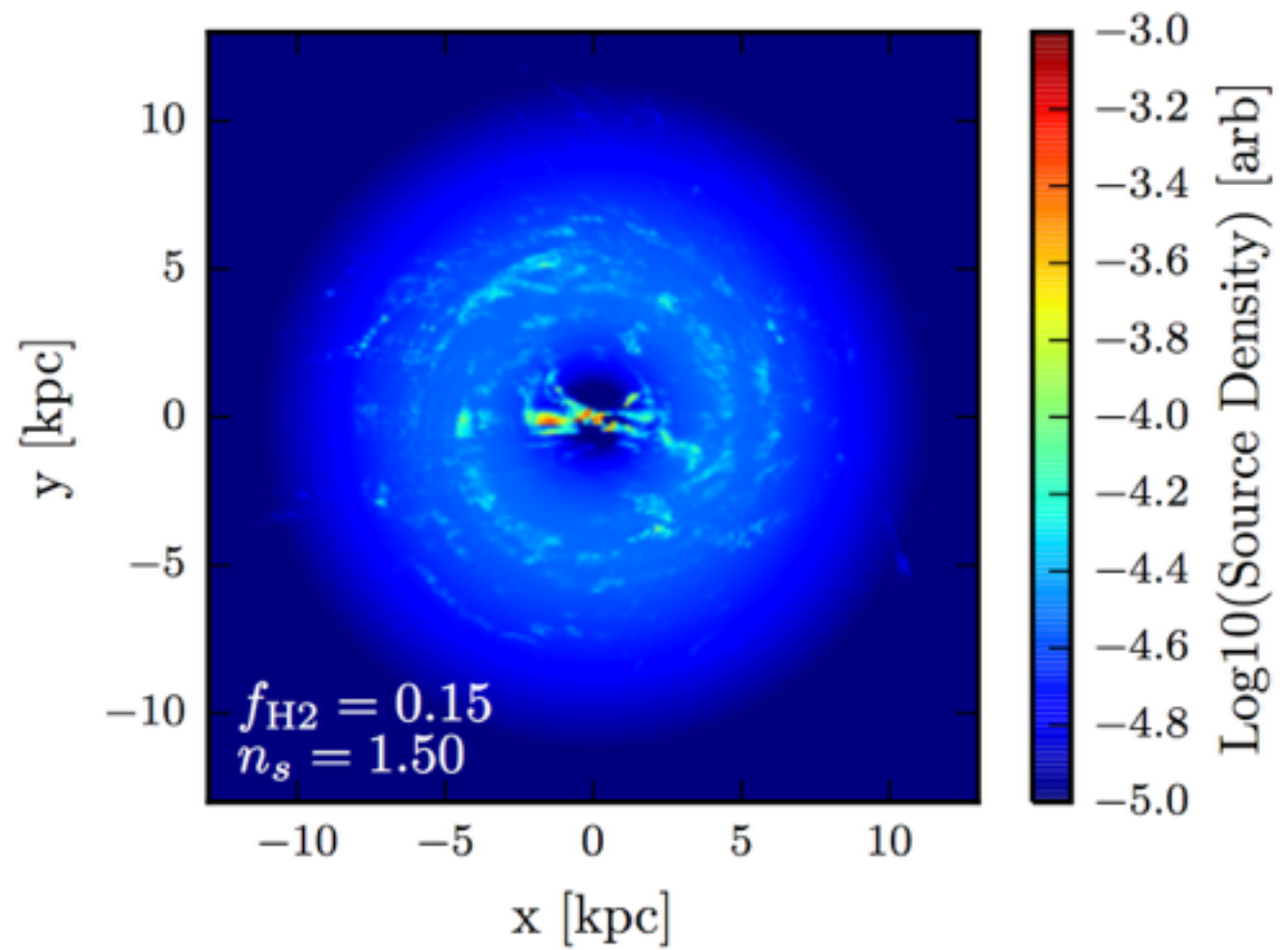
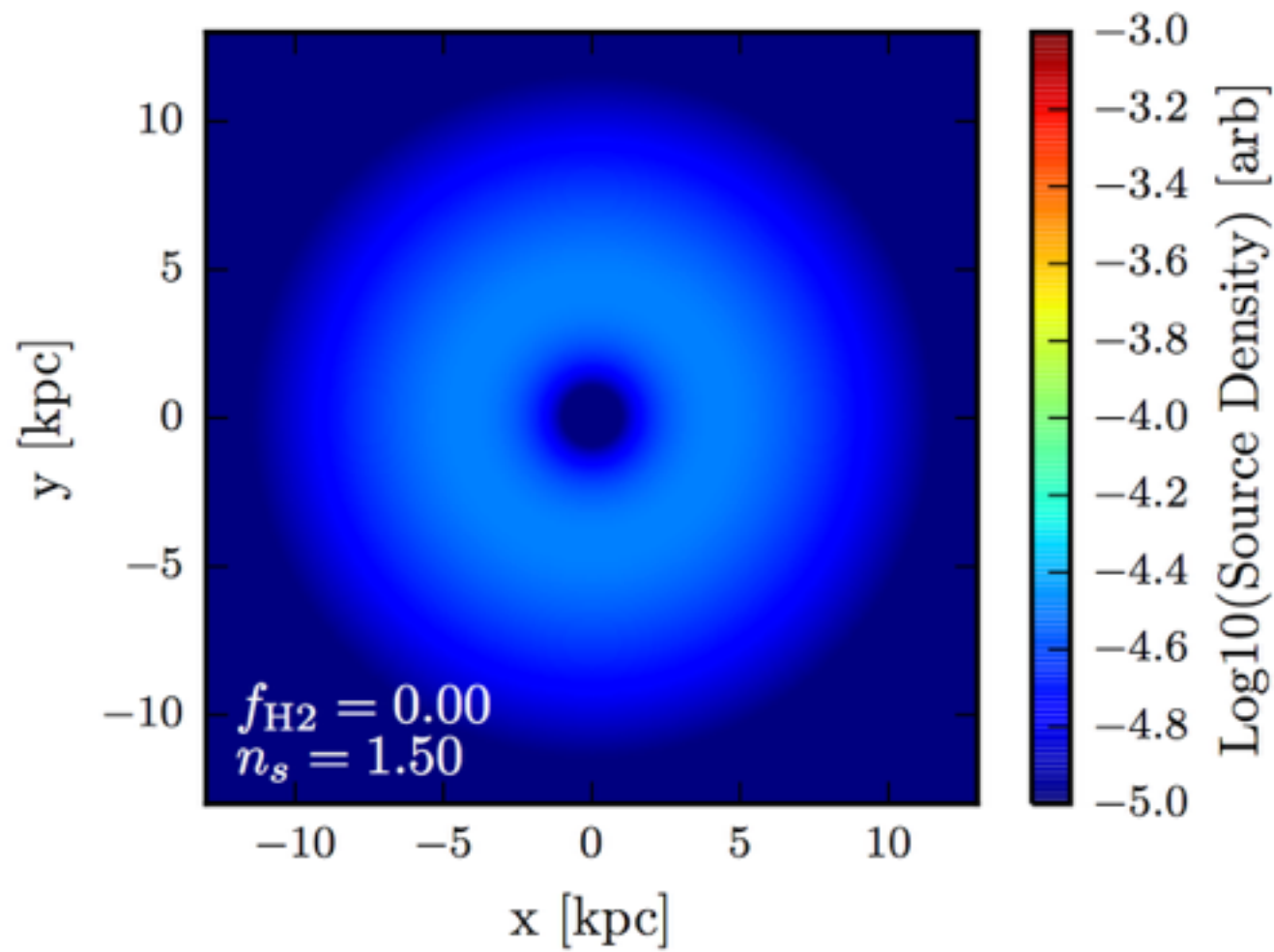
Theoretically Motivated: Molecular Gas is the seed of star formation, the Schmidt Law gives

$$\Sigma_{\text{SFR}} \propto \Sigma_{\text{Gas}}^{1.4 \pm .15}$$

Specifically we inject a fraction of cosmic-rays (f_{H_2}) following:

$$Q_{\text{CR}}(\vec{r}) \propto \begin{cases} 0 & \rho_{\text{H}_2} \leq \rho_s \\ \rho_{\text{H}_2}^{n_s} & \rho_{\text{H}_2} > \rho_s \end{cases}$$

The Solution

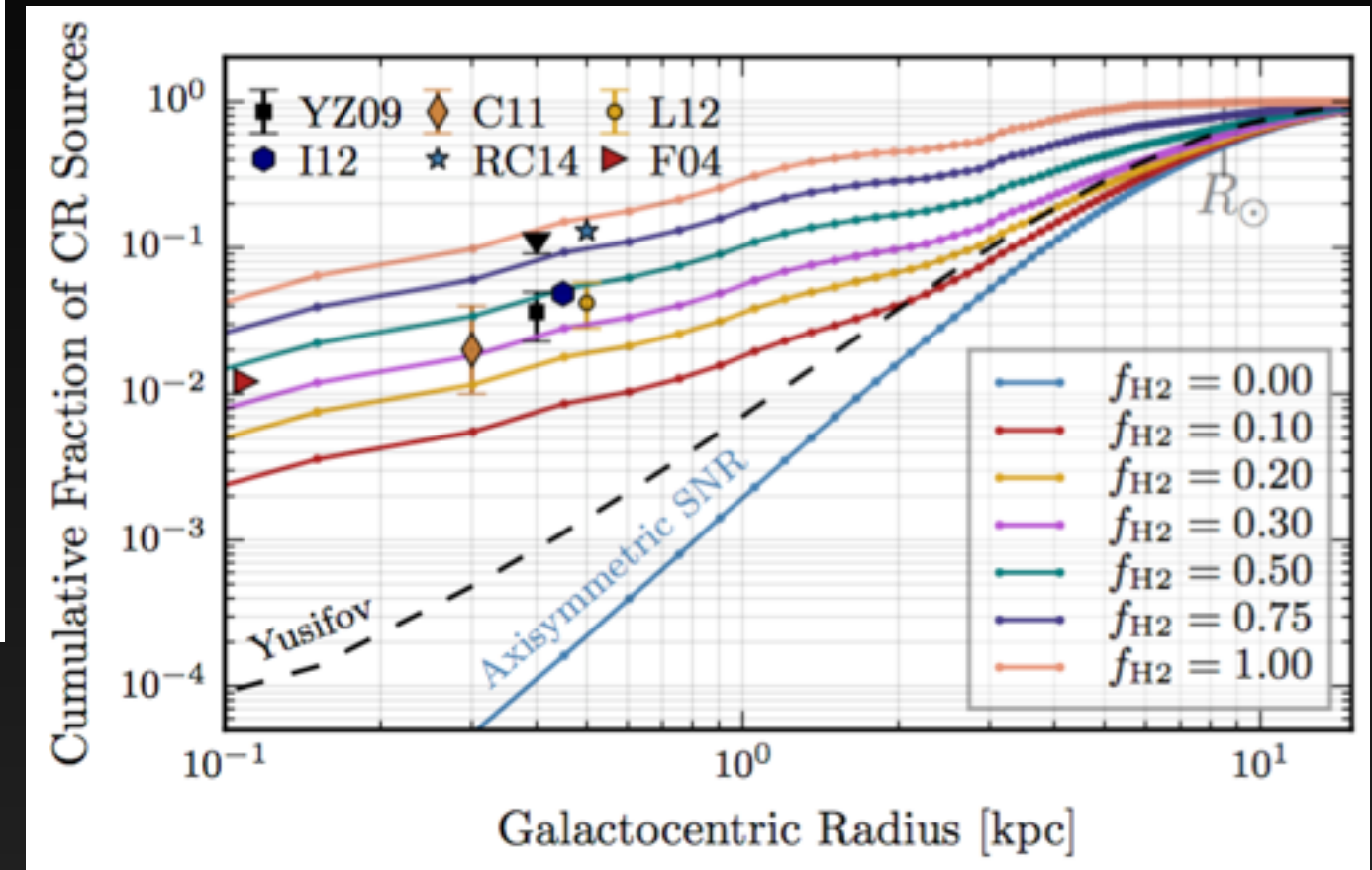
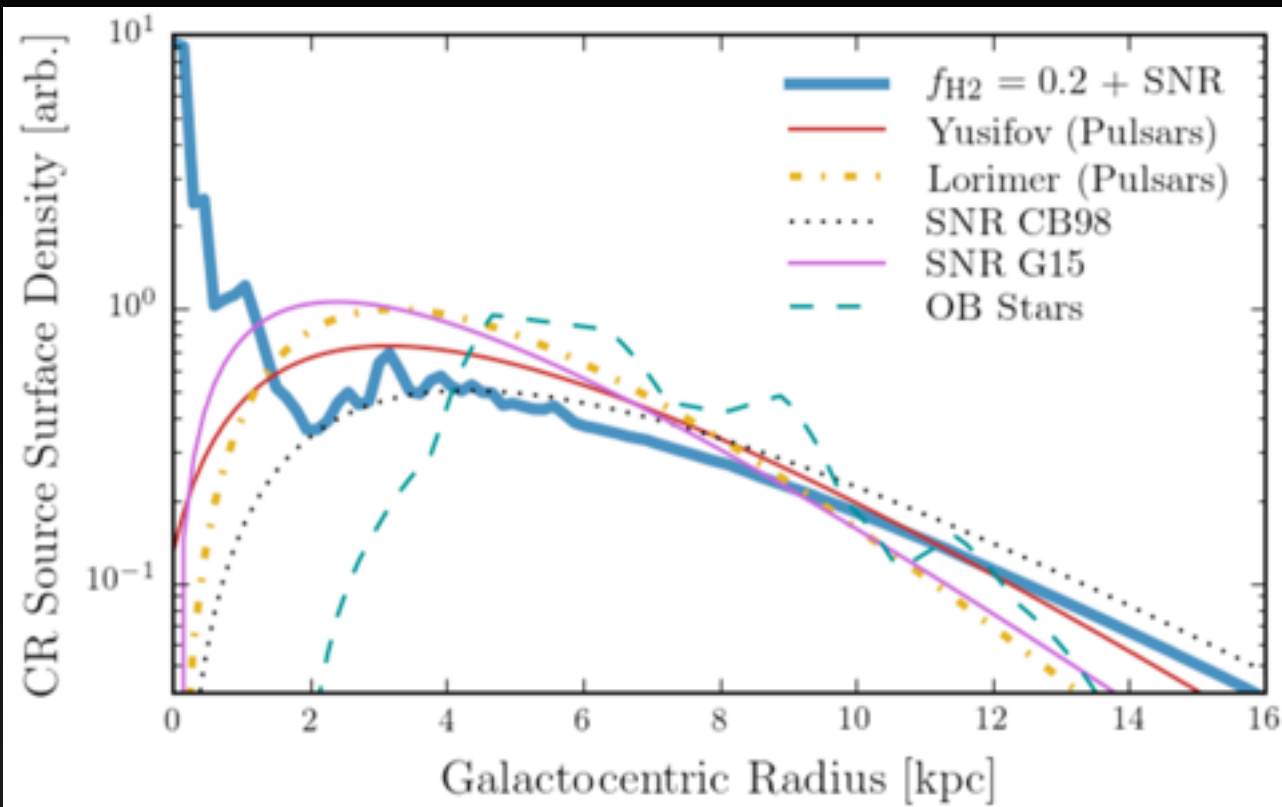


Two features leap out immediately:

1.) Spiral Arms

2.) A bright bar in the Galactic Center

The Solution



Adds a new, and significant, cosmic-ray injection component, in particular near the Galactic Center.

The cosmic-ray injection rate now matches observational constraints.

Simulations!

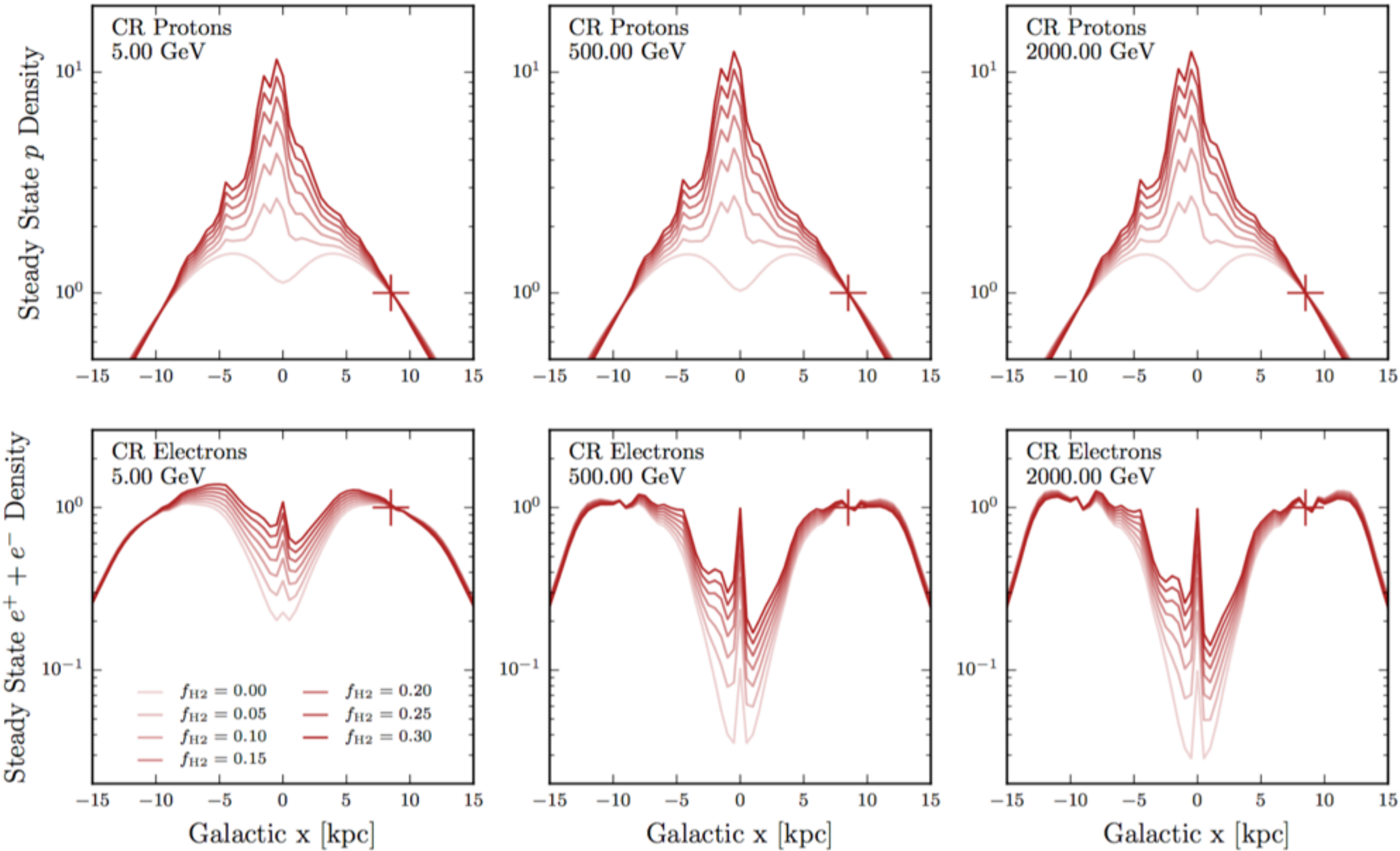
| Parameter | Units | Canonical | Mod A | Description |
|-------------------|-------------------------------------|----------------------|----------------------|---|
| D_0 | $\text{cm}^2 \text{ s}^{-1}$ | 7.2×10^{28} | 5.0×10^{28} | Diffusion constant at $\mathcal{R} = 4 \text{ GV}$ |
| δ | — | 0.33 | 0.33 | Index of diffusion constant energy dependence |
| z_{halo} | kpc | 3 | 4 | Half-height of diffusion halo |
| R_{halo} | kpc | 20 | 20 | Radius diffusion halo |
| v_a | km s^{-1} | 35 | 32.7 | Alfvén velocity |
| dv/dz | $\text{km s}^{-1} \text{ kpc}^{-1}$ | 0 | 50 | Vertical convection gradient |
| α_p | — | 1.88 (2.39) | 1.88 (2.47) | p injection index below (above) $\mathcal{R} = 11.5 \text{ GV}$ |
| α_e | — | 1.6 (2.42) | 1.6 (2.43) | e^- injection index below (above) $\mathcal{R} = 2 \text{ GV}$ |
| Source | — | SNR | SNR | Distribution of $(1 - f_{\text{H}_2})$ primary sources* |
| f_{H_2} | — | .20 | N/A | Fraction of sources in star formation model* |
| n_s | — | 1.5 | N/A | Schmidt Index* |
| ρ_c | cm^{-3} | 0.1 | N/A | Critical H_2 density for star formation* |
| B_0 | μG | 7.2 | 9.0 | Local ($r = R_\odot$) magnetic field strength |
| r_B, z_B | kpc | 5, 1 | 5, 2 | Scaling radius and height for magnetic field |
| ISRF | — | (1.0,.86,.86) | (1.0,.86,.86) | Relative CMB, Optical, FIR density |
| dx, dy | kpc | 0.5, 0.5 | 1 (2D) | x, y (3D) or radial (2D) cosmic-ray grid spacing |
| dz | kpc | 0.125 | .1 | z-axis cosmic-ray grid spacing |

Add the new cosmic-ray injection models into Galprop.

CO ratios are fitted in galactocentric rings to produce a full sky model (Ackermann et al. 2012)

| Ring Number | Radius [kpc] | Fit Region | X_{CO} [$\text{cm}^{-2} (\text{K km s}^{-1})^{-1}$] |
|-------------|--------------|------------|--|
| 1 | 0 – 2.0 | Inner | $1.00 \times 10^{19}\dagger$ |
| 2 | 2.0 – 3.0 | Inner | 8.42×10^{19} |
| 3 | 3.0 – 4.0 | Inner | 1.61×10^{20} |
| 4 | 4.0 – 5.0 | Inner | 1.73×10^{20} |
| 5 | 5.0 – 6.5 | Inner | 1.72×10^{20} |
| 6 | 6.5 – 8.0 | Inner | 1.74×10^{20} |
| 7 | 8.0 – 10.0 | Local | 8.61×10^{19} |
| 8 | 10.0 – 16.5 | Outer | 4.29×10^{20} |
| 9 | 16.5 – 50.0 | Outer | 2.01×10^{21} |

Steady State Cosmic-Ray Distribution

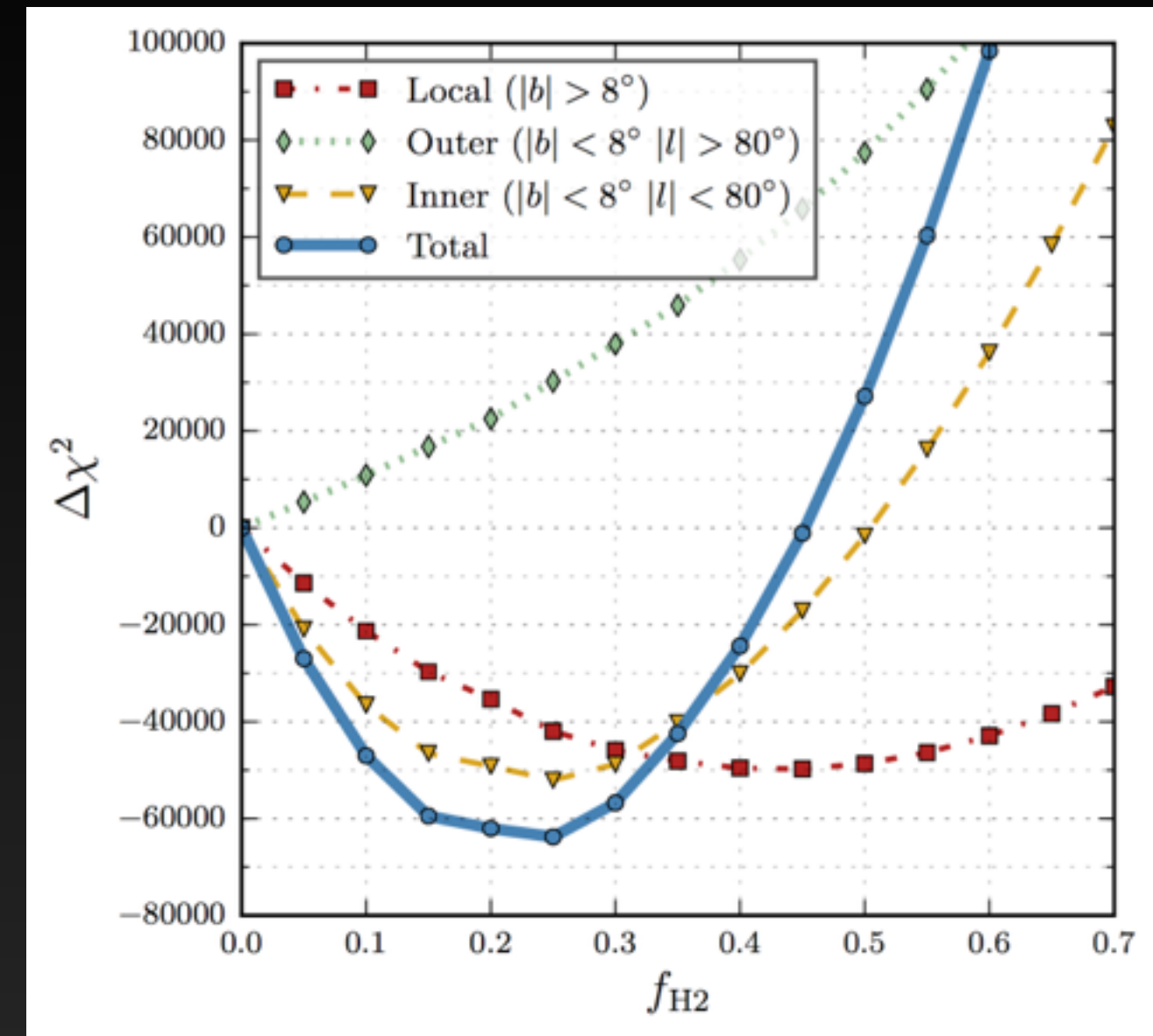


A Better fit to the Gamma-Ray Sky

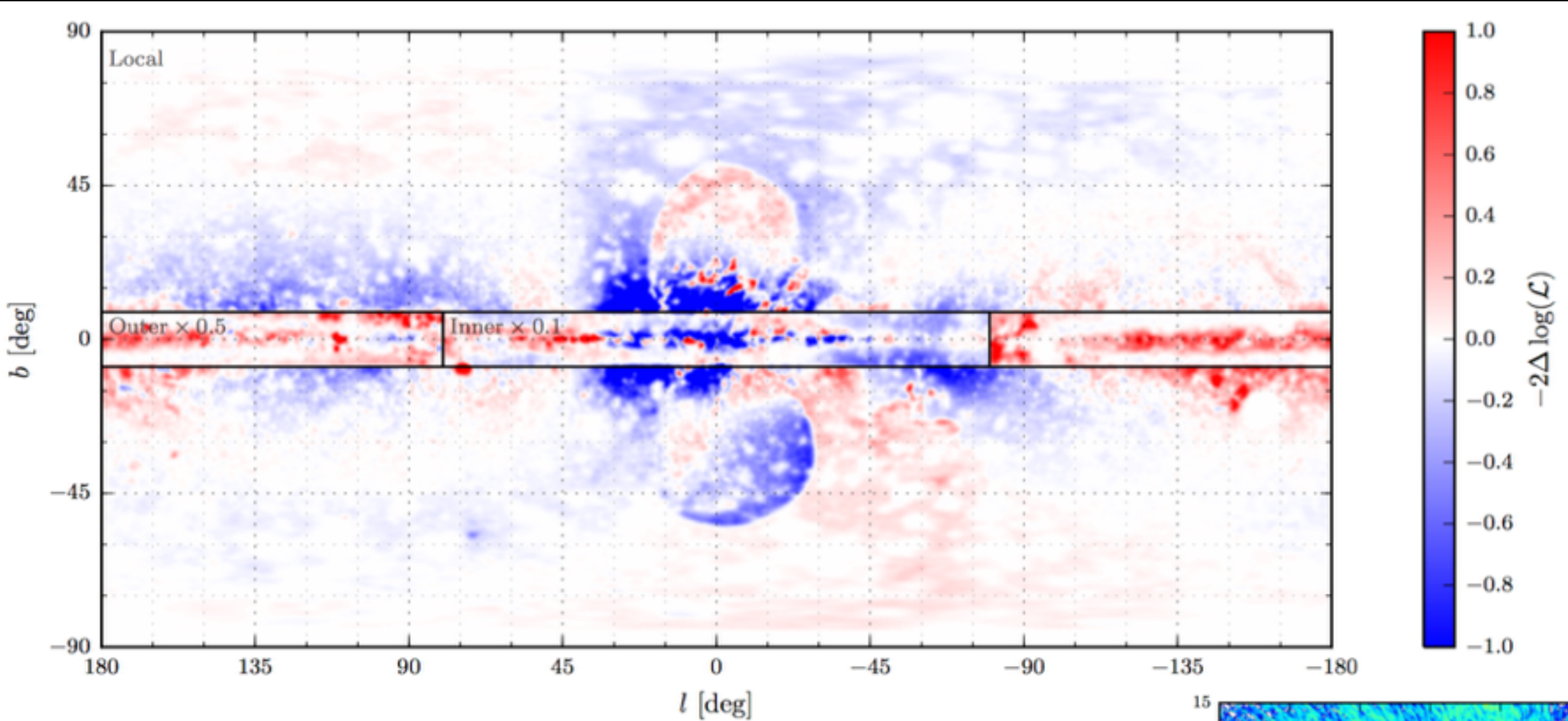
1.) The addition of a new cosmic-ray injection template tracing the 3D H₂ density greatly improves the overall fit to the gamma-ray diffuse emission.

2.) This is an important point on its own, as it offers a new method for improving diffuse models for the gamma-ray sky.

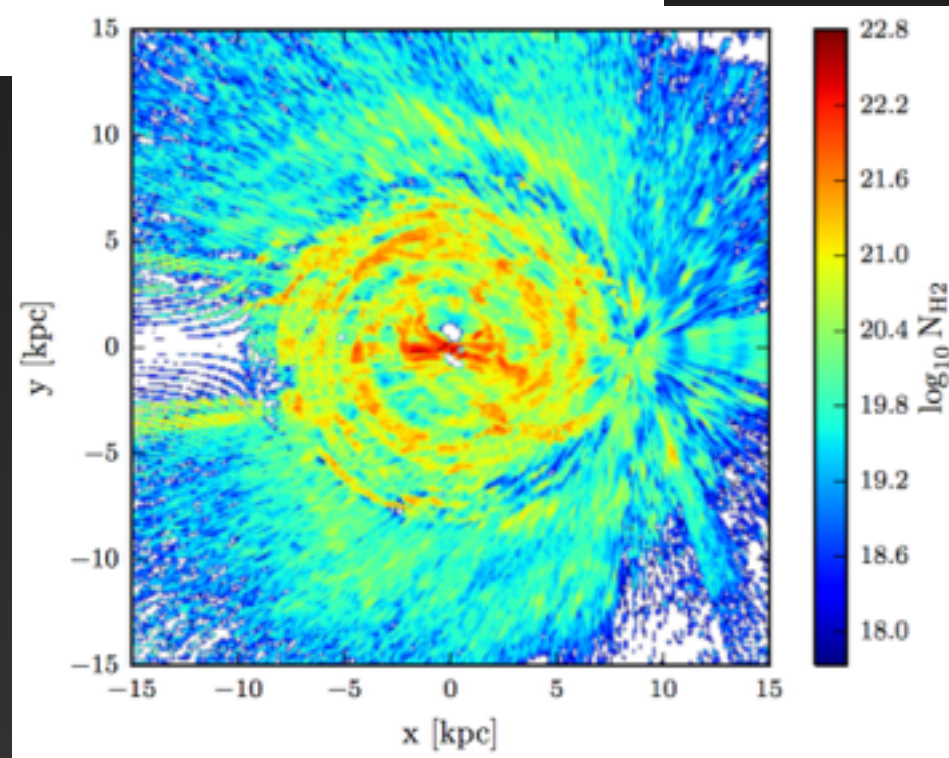
3.) Technique will become more powerful with the introduction of 3D gas and dust maps in the near future.



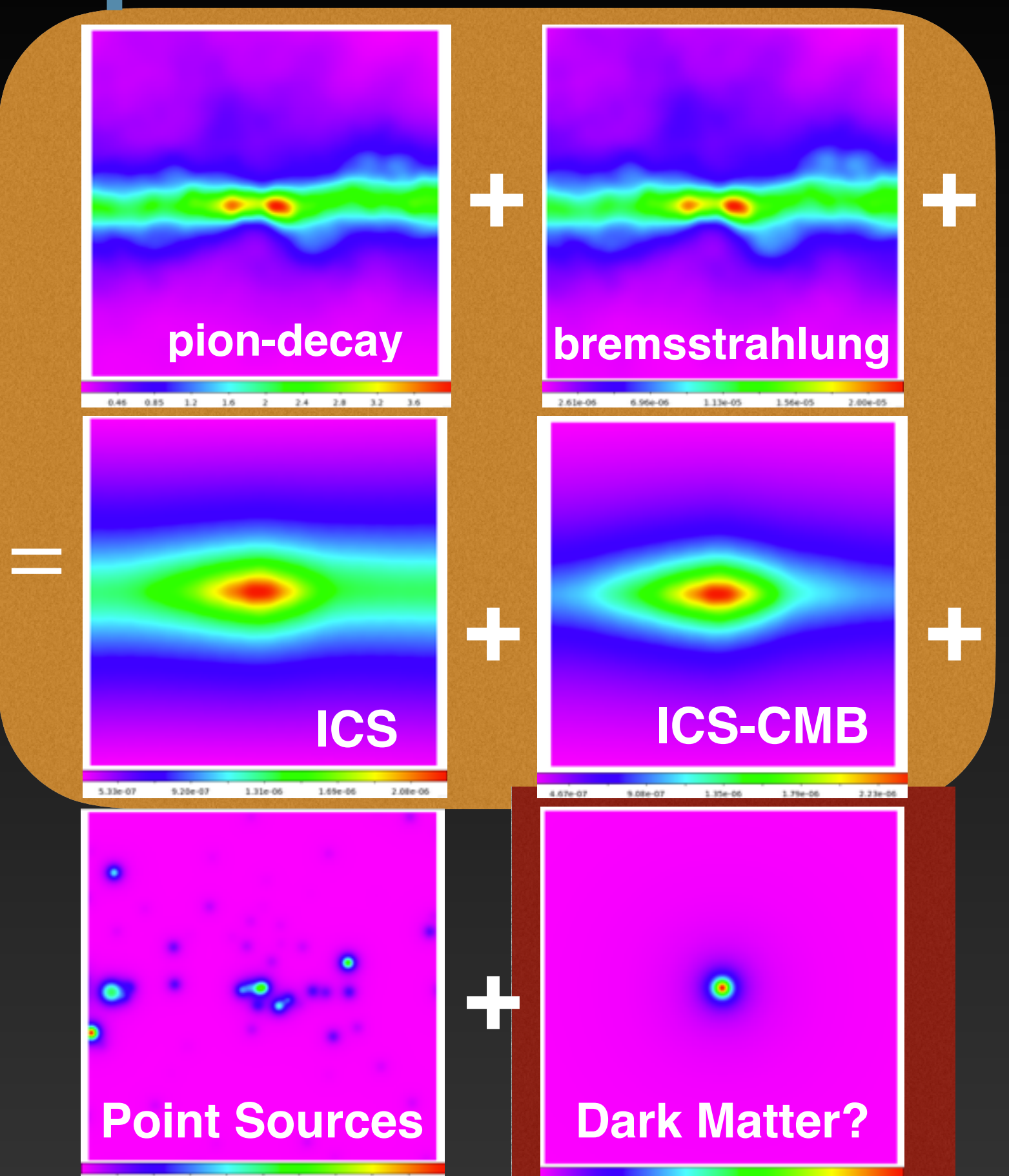
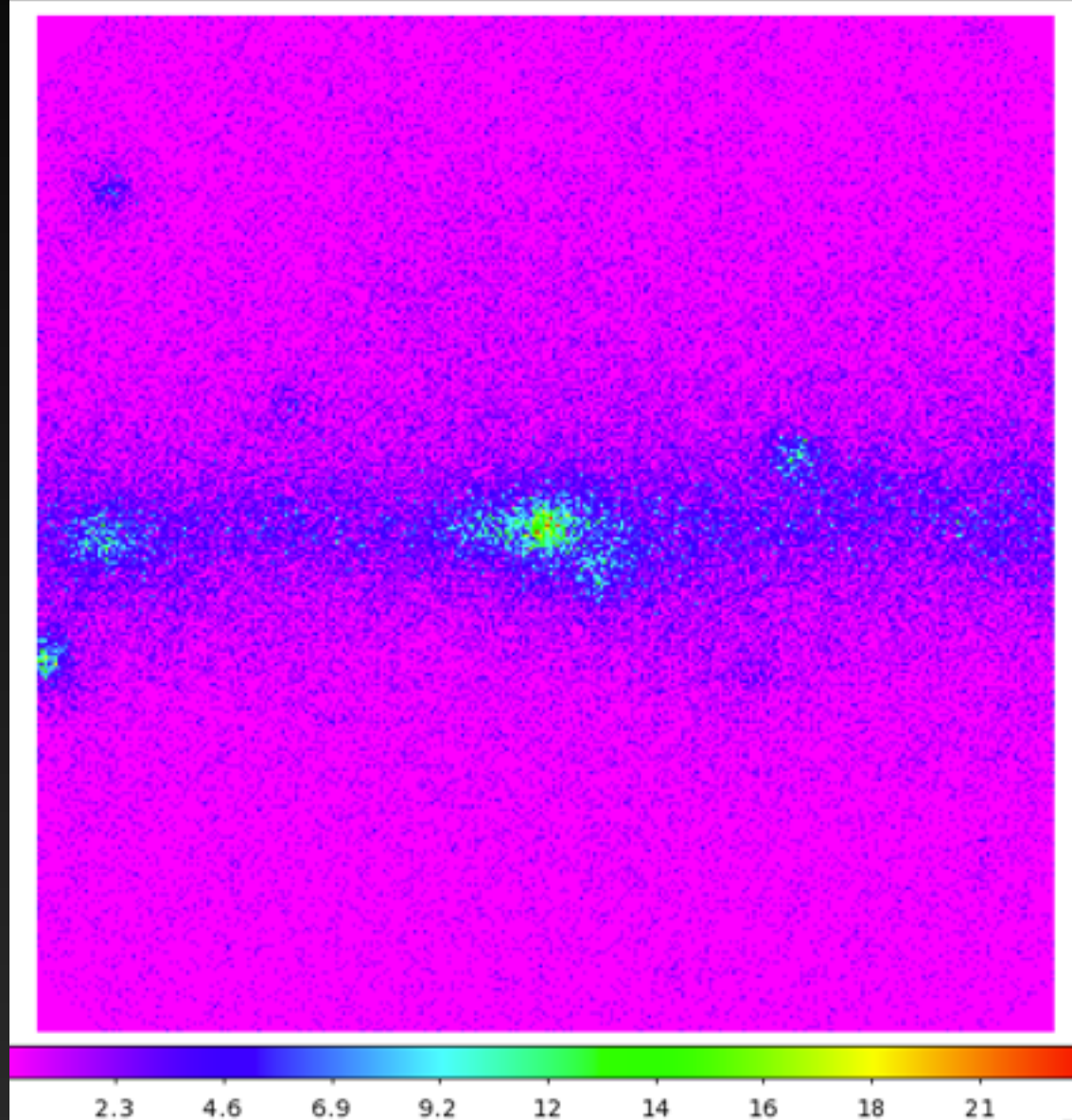
A Better fit to the Gamma-Ray Sky



Fits are significantly improved, in particular in regions near the Galactic Center where there is significant kinematic gas information.



Untangling the spider's web



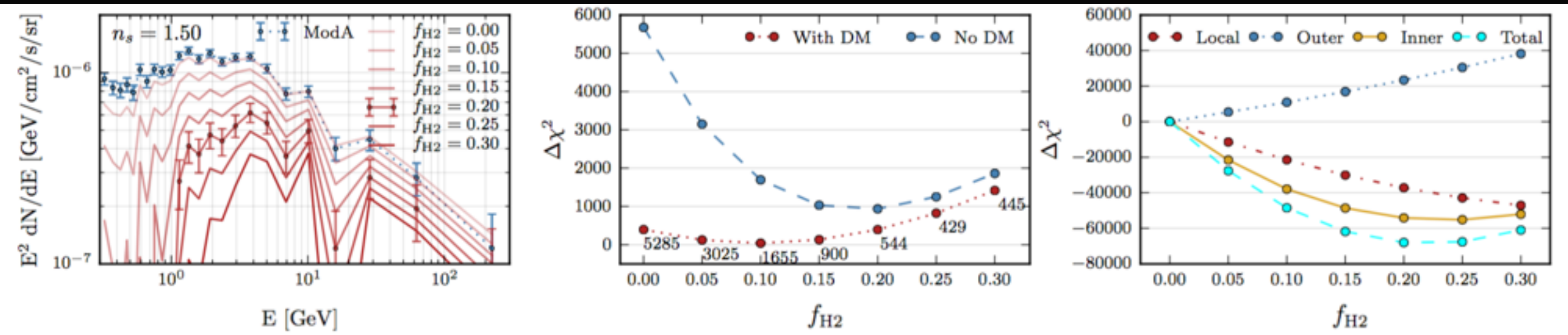
An Inner Galaxy Analysis of the GCE

INNER GALAXY

- Mask galactic plane (e.g. $|b| > 2^\circ$), and consider $40^\circ \times 40^\circ$ box
- Energy dependent masking of bright point sources (following Calore et al. 2014)
- Use likelihood analysis, allowing the diffuse templates to float in each energy bin
 - Isotropic energy spectrum fixed via error bars in EGRB analysis (Fermi-LAT 2014)
 - Bubbles fixed via error bars from Su et al.

This creates an analysis with a large sidebands region, where the best fit normalization of the diffuse components is relatively independent of the NFW template.

Effect on the Gamma-Ray Excess



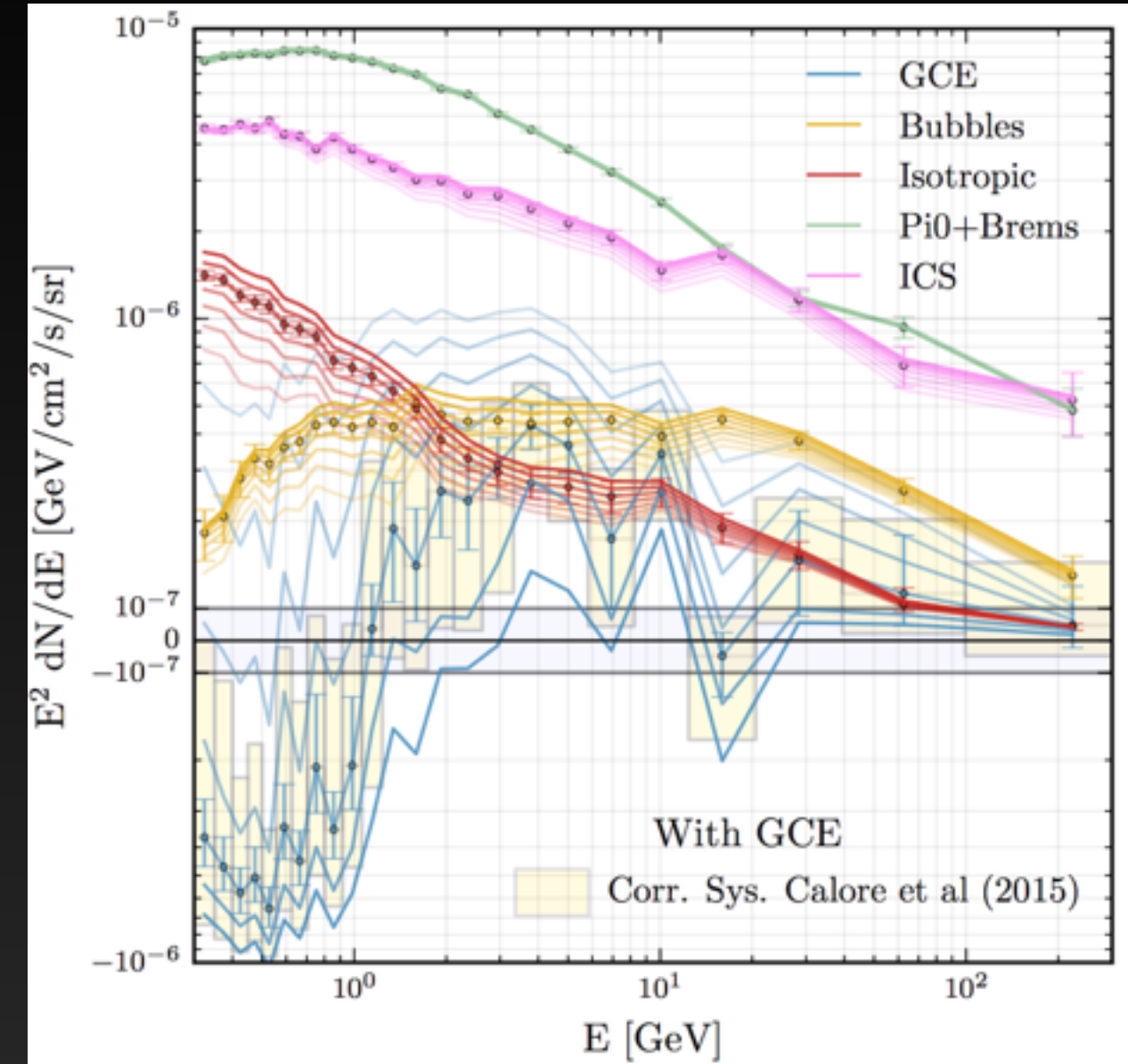
The inclusion of a diffuse emission template tracing the H₂ density significantly decreases the intensity of the gamma-ray excess.

However, in the best global fit to the data, the value of f_{H2} decreases to 0.1, and the intensity of the GC excess decreases by only ~30%.

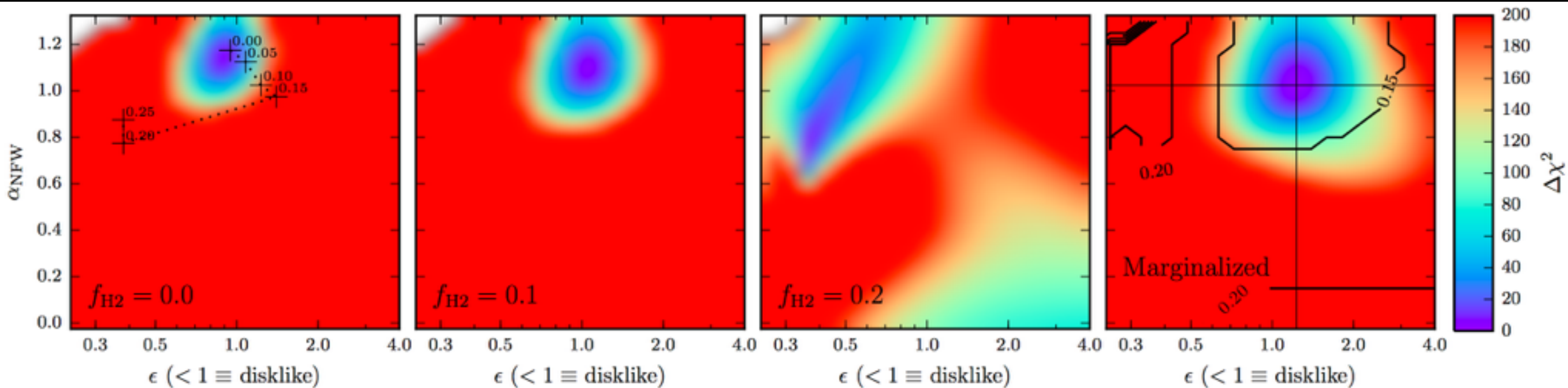
Effect on the Excess Spectrum

Changing the morphology of the excess has a significant effect on the spectrum of the gamma-ray excess.

The spectrum becomes extremely hard as f_{H_2} is increased, most likely indicating that the GCE template is picking up mismodeling of some residual.



Effect on the Excess Morphology



The morphology of the Gamma-Ray Excess is also degenerate with the value of $f_{\text{H}2}$.

As $f_{\text{H}2}$ is increased, the best-fit morphology becomes stretched perpendicular to the galactic plane.

However, marginalized over all values of $f_{\text{H}2}$, the standard NFW template is still consistent with the data.

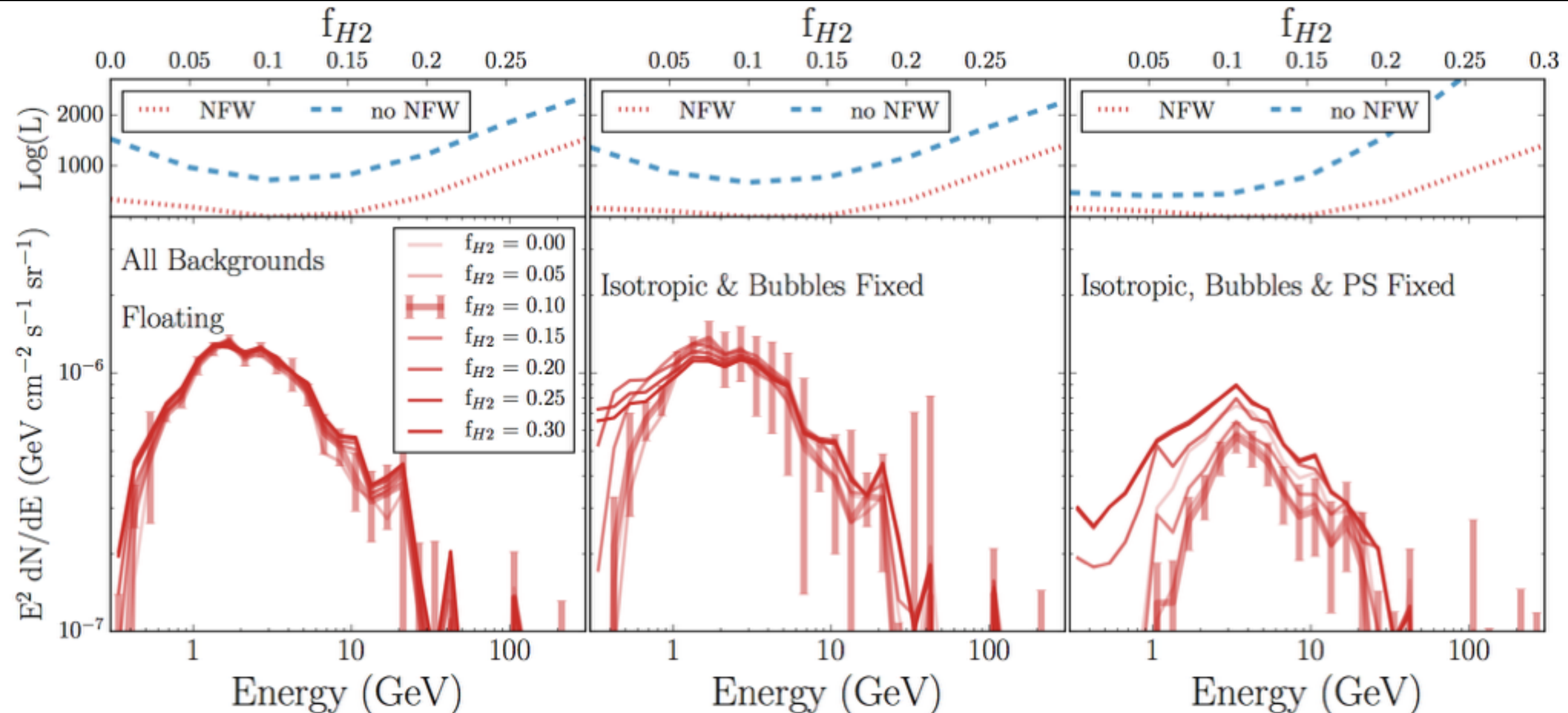
A Galactic Center Analysis of the GCE

GALACTIC CENTER

- Examine $15^\circ \times 15^\circ$ region surrounding the galactic center.
- No point source masking
- Use likelihood analysis, allowing the diffuse templates and point sources to float in each energy bin.

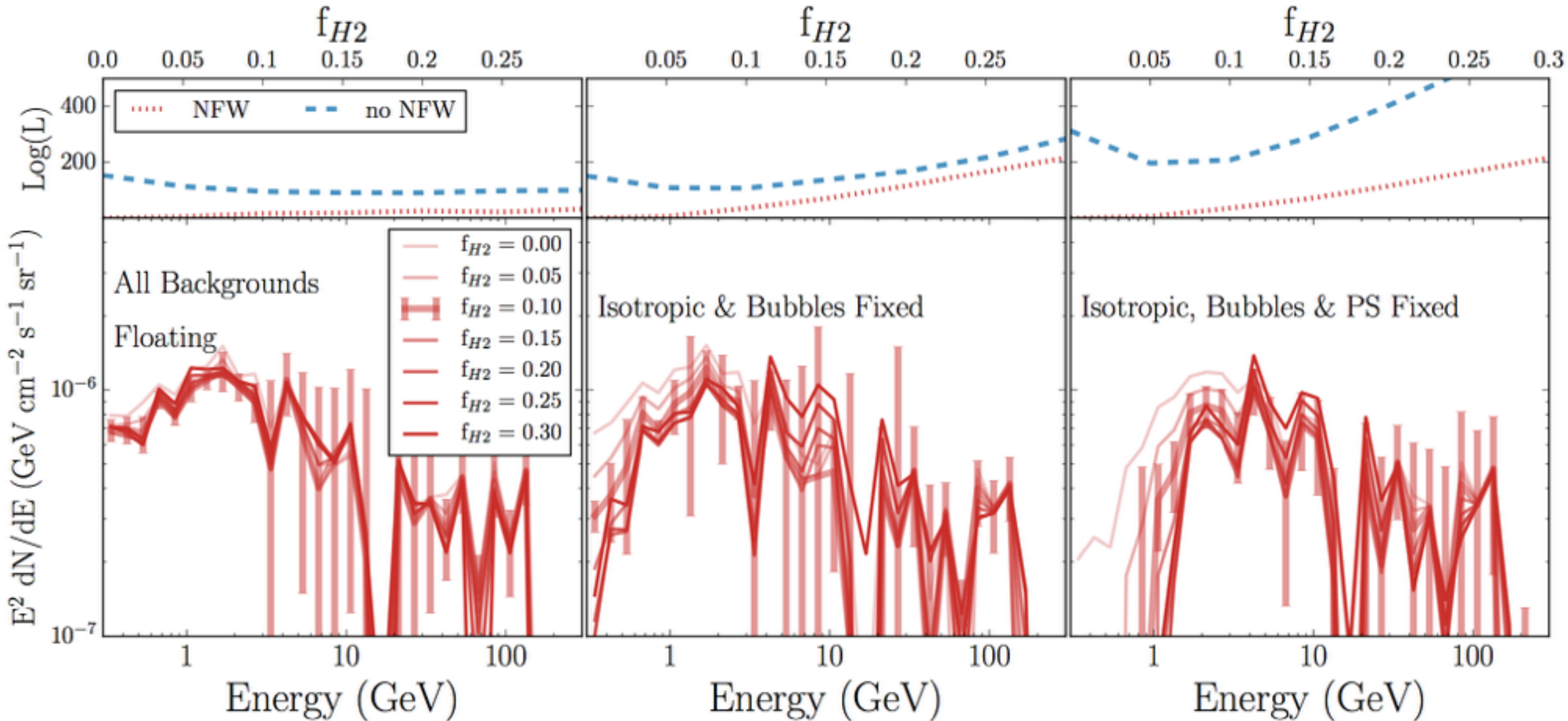
This creates an analysis with no sidebands region, where the NFW template normalization plays a critical role in determining the spectrum and normalization of diffuse components.

The Effect on the Galactic center Excess



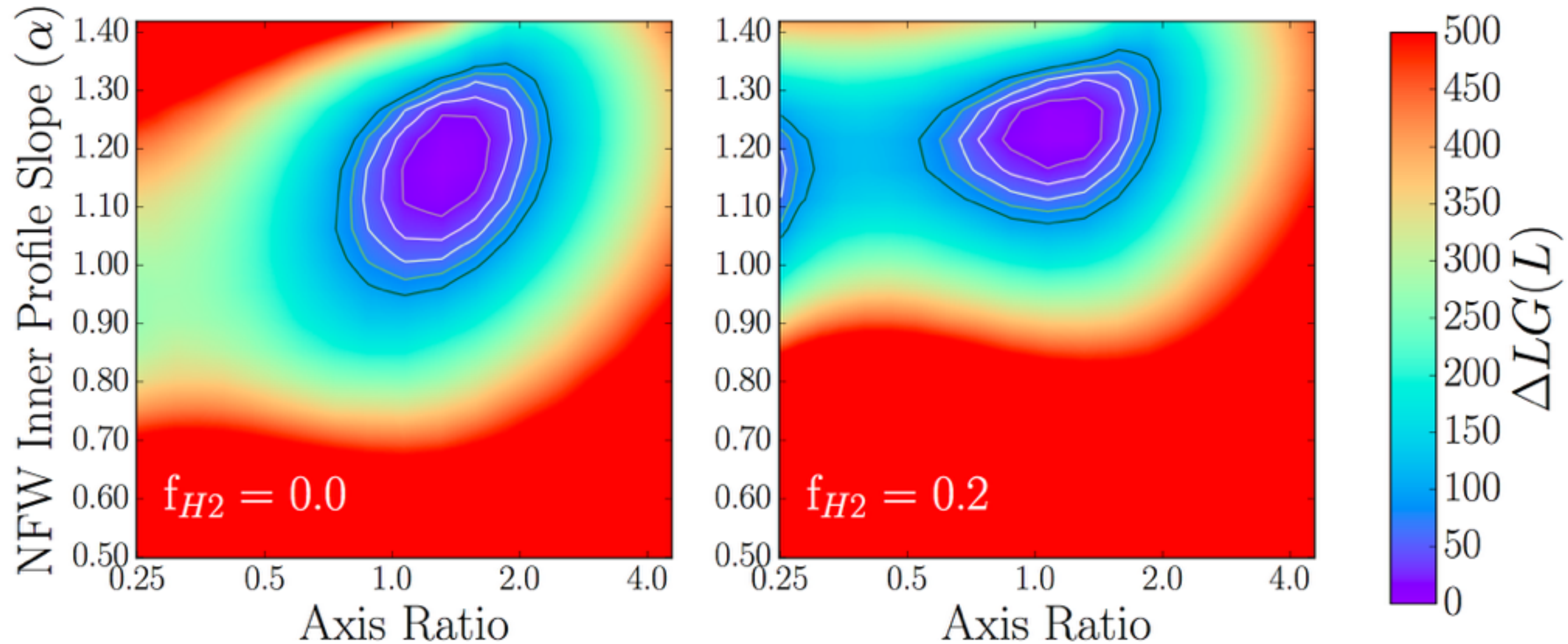
In this smaller region, the excess remains resilient to changes in diffuse emission modeling.

The Effect on the Galactic center Excess (masking $|b| < 2^\circ$)



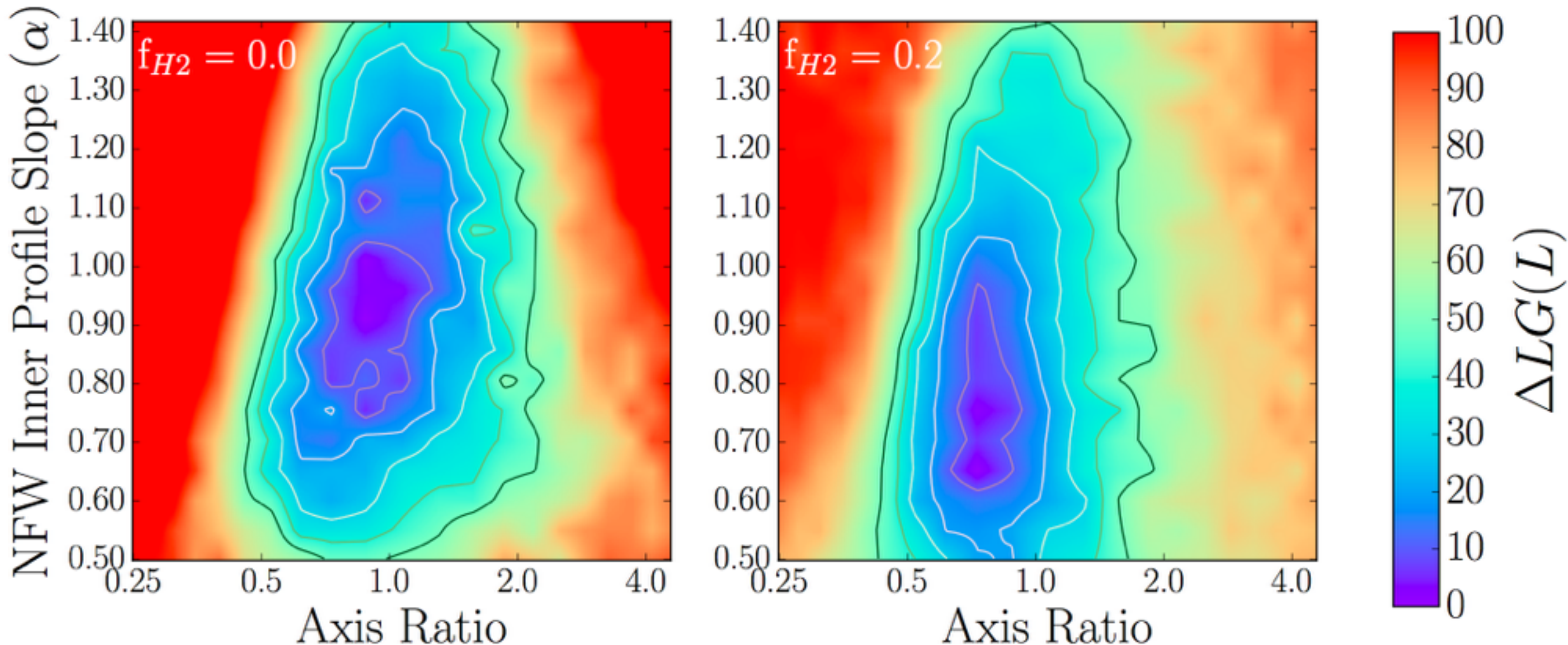
Intriguingly, this persists even when the inner 2° are masked - implying that analyses of small ROIs favors the excess.

The Galactic Center Excess Morphology



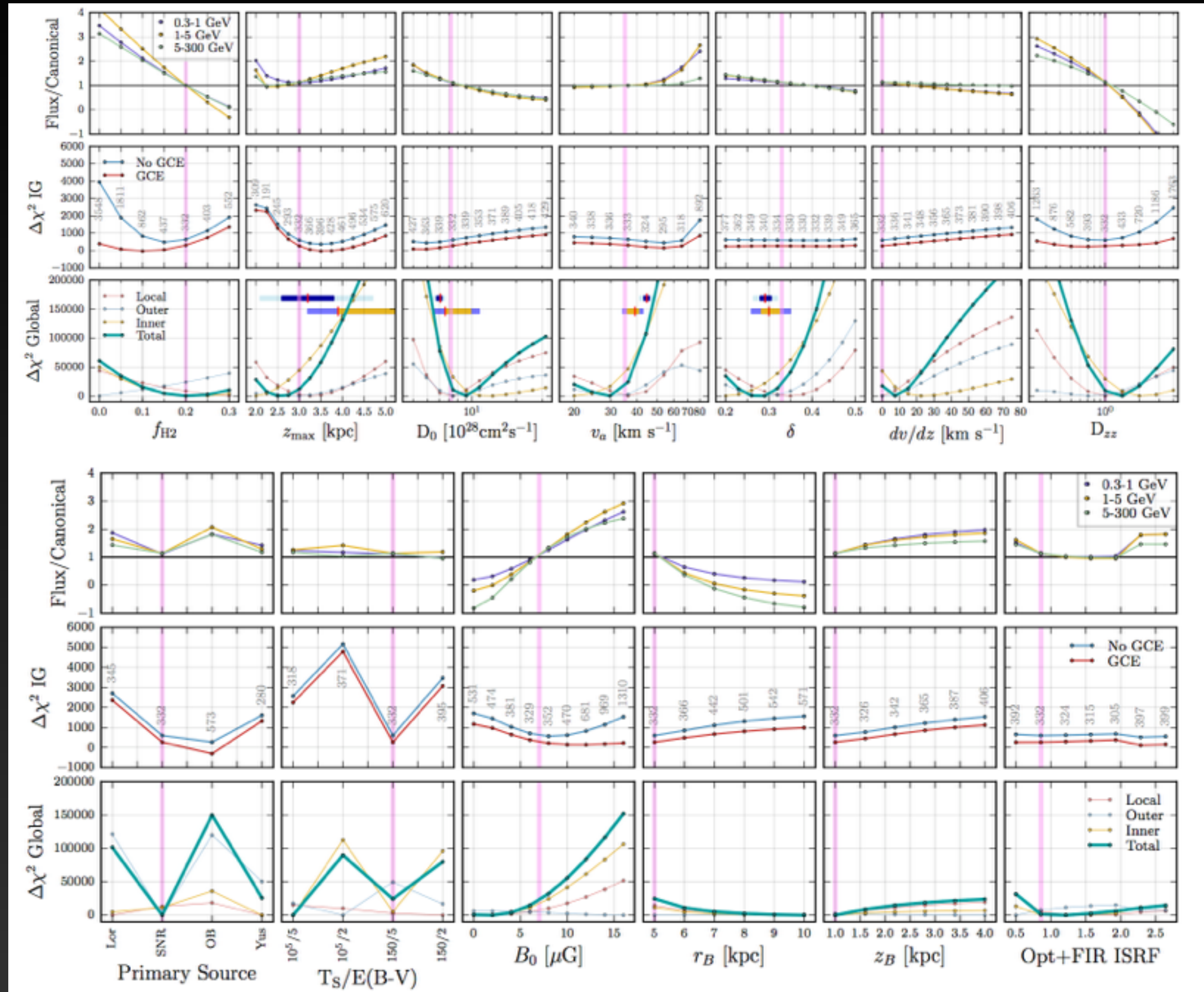
For the Galactic Center analysis, the morphology of the excess component remains relatively robust

The Galactic Center Excess Morphology (masking $|b| < 2^\circ$)

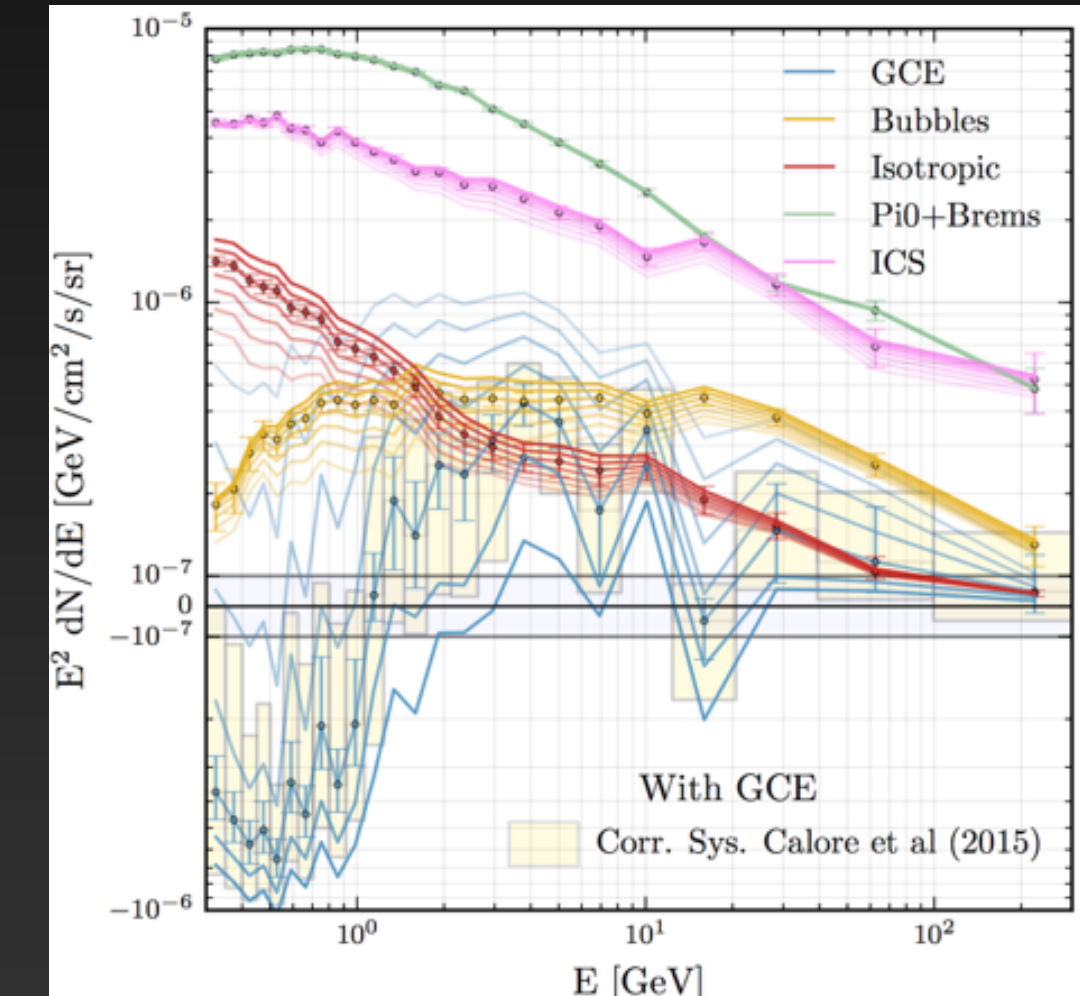
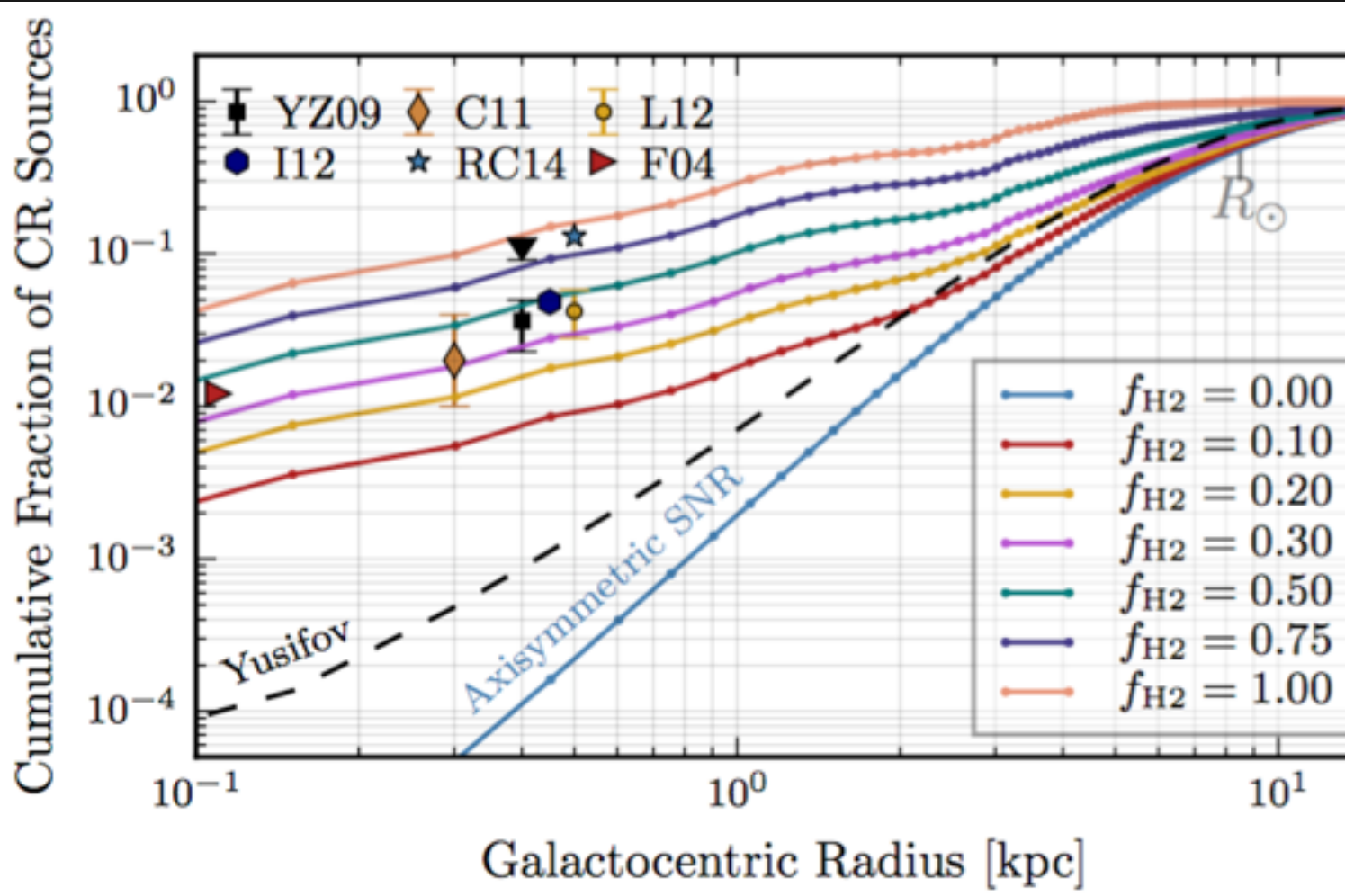
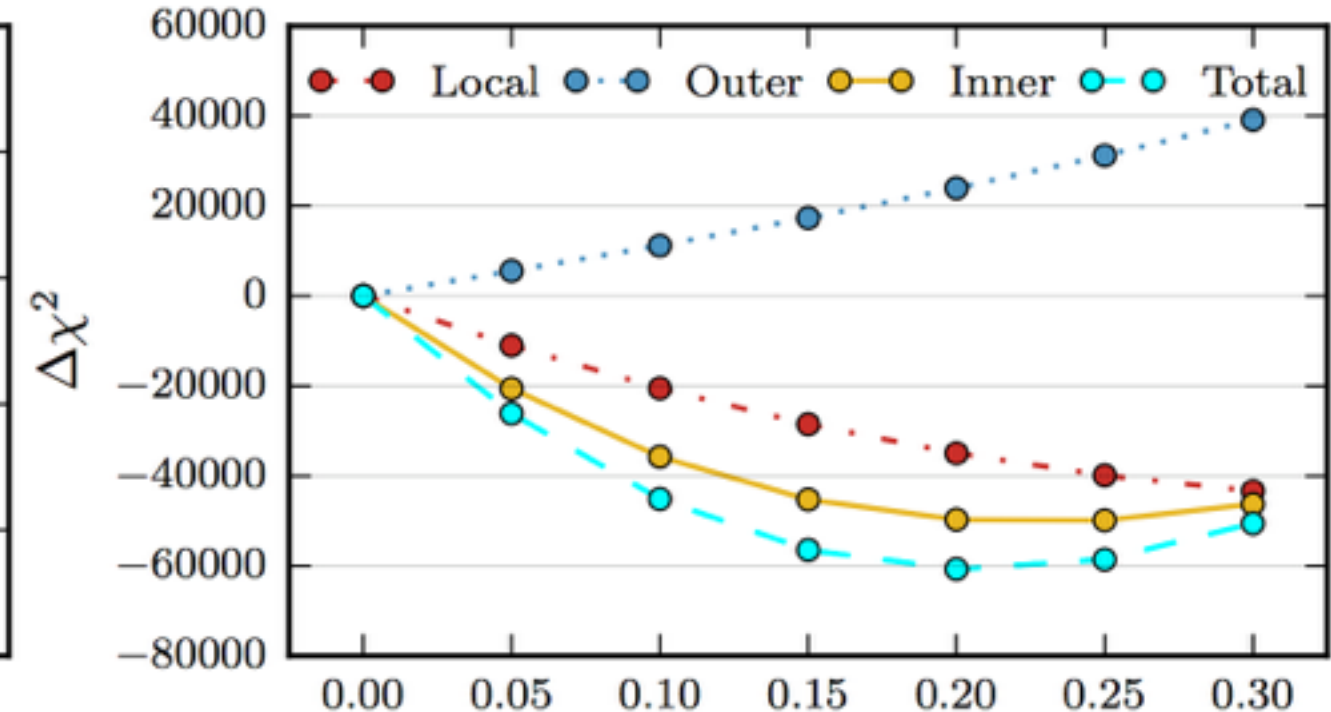
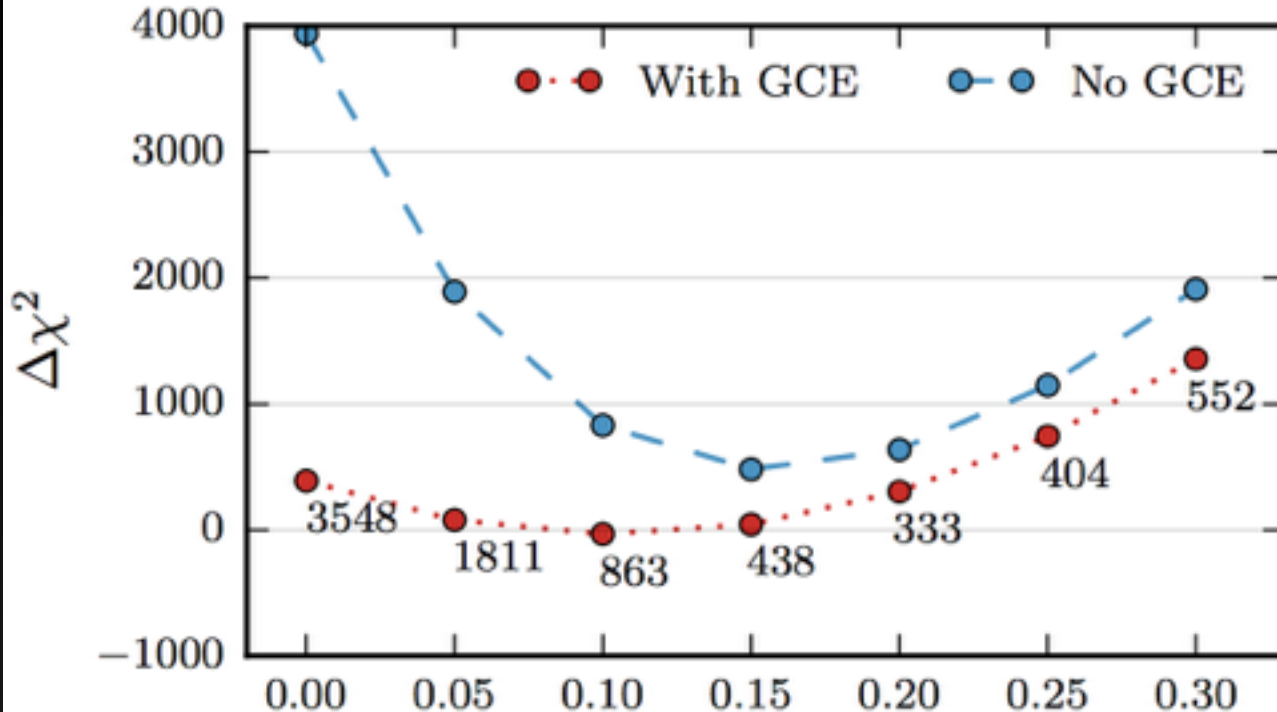


The deviations from typical NFW profiles are more extreme when the $|b| < 2^\circ$ is masked from the analysis, with a shallower emission profile preferred by the data.

Galactic center excess is resilient to many other parameters....



The Galactic Center Deficit?

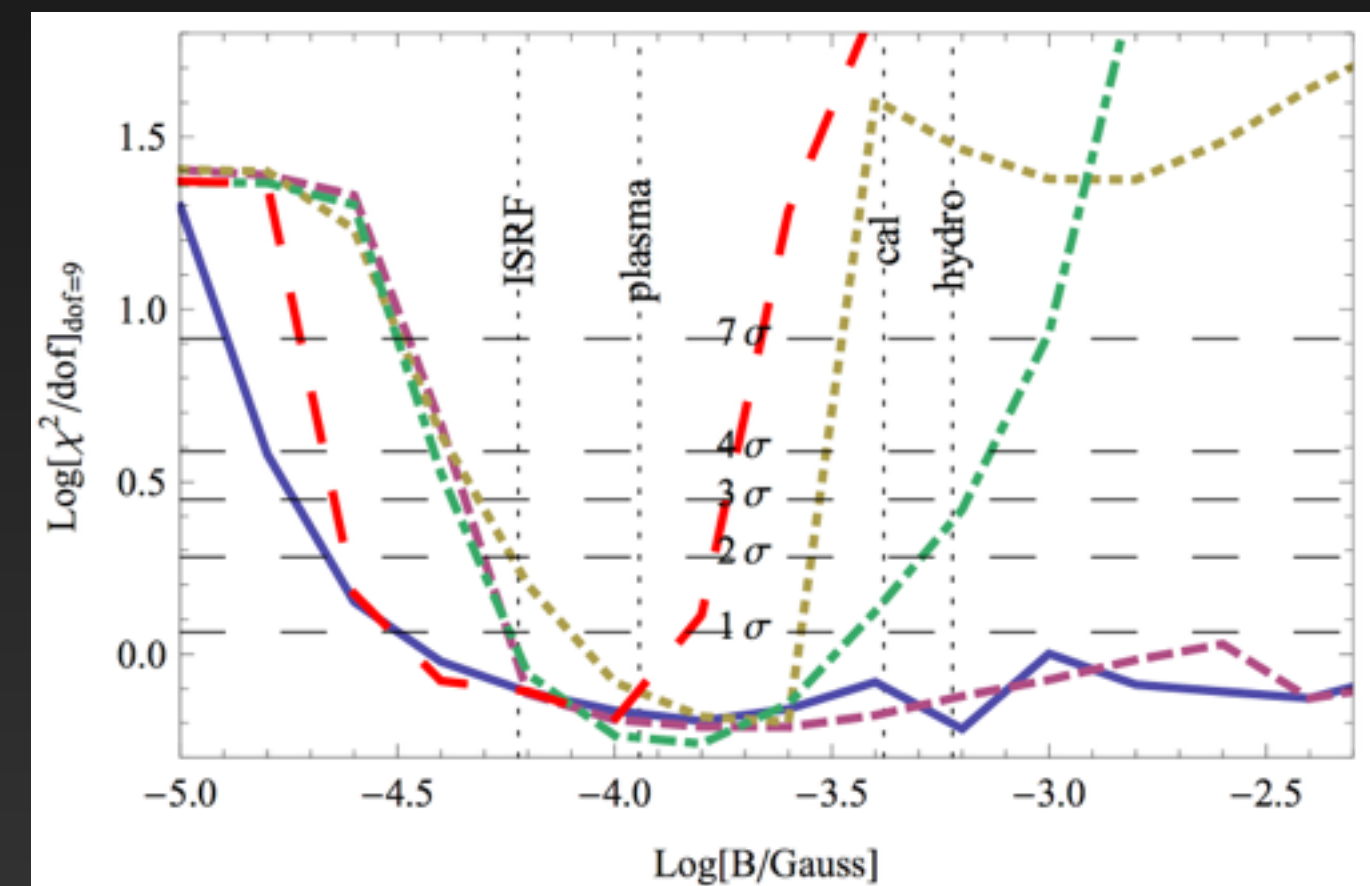
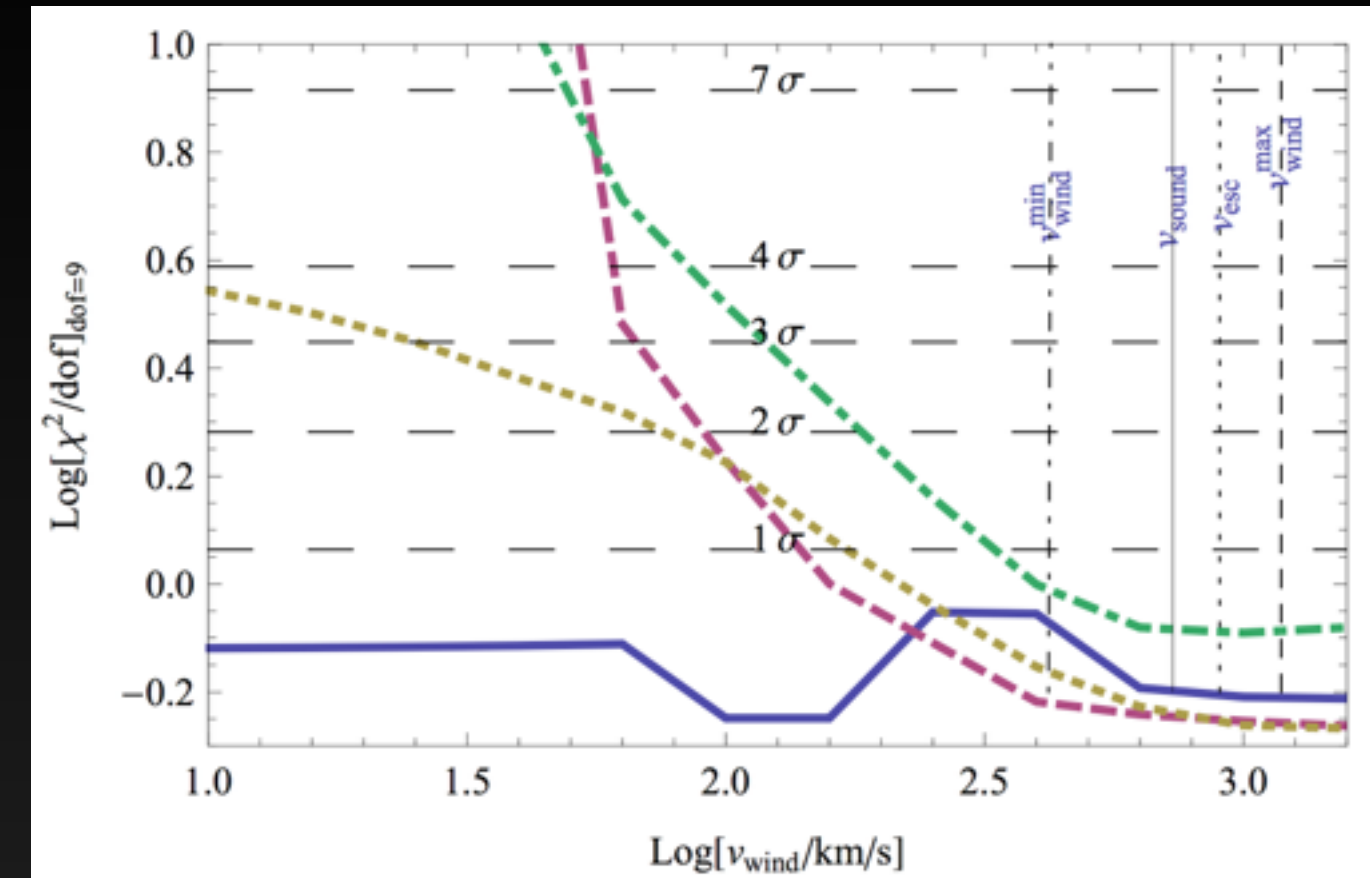


Advection and Convection in the Galactic Center

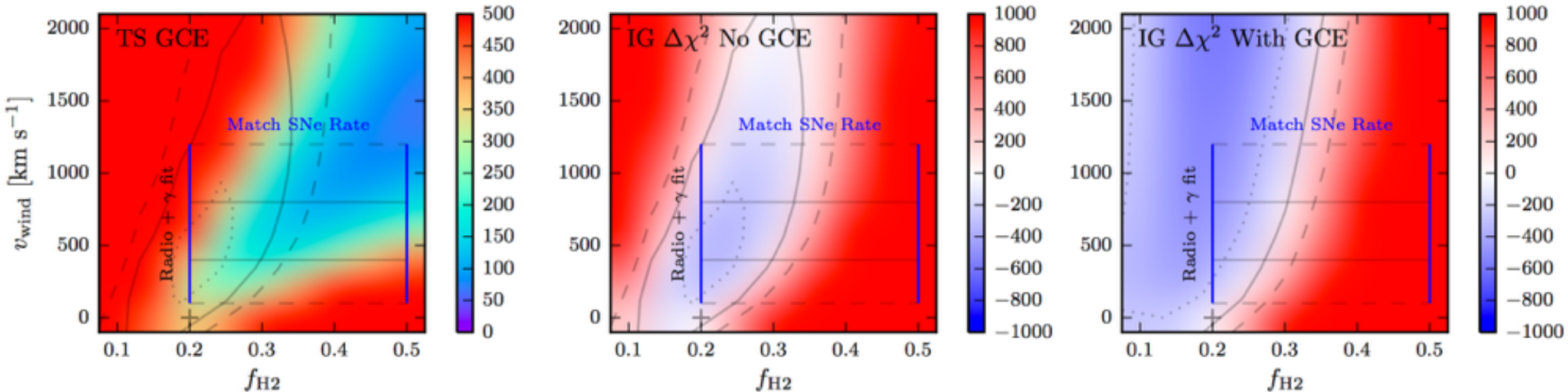
Crocker et al. (2011) demonstrated that the break in the GC synchrotron spectrum is best fit in the regime with:

- a.) Large Magnetic Fields
- b.) Large Convective Winds

Very different from typical Galprop diffusion scenario.



Convection in the Galactic Center



This increases the best fit value of f_{H_2} for the GC data, bringing this value into agreement with the global best fit value.

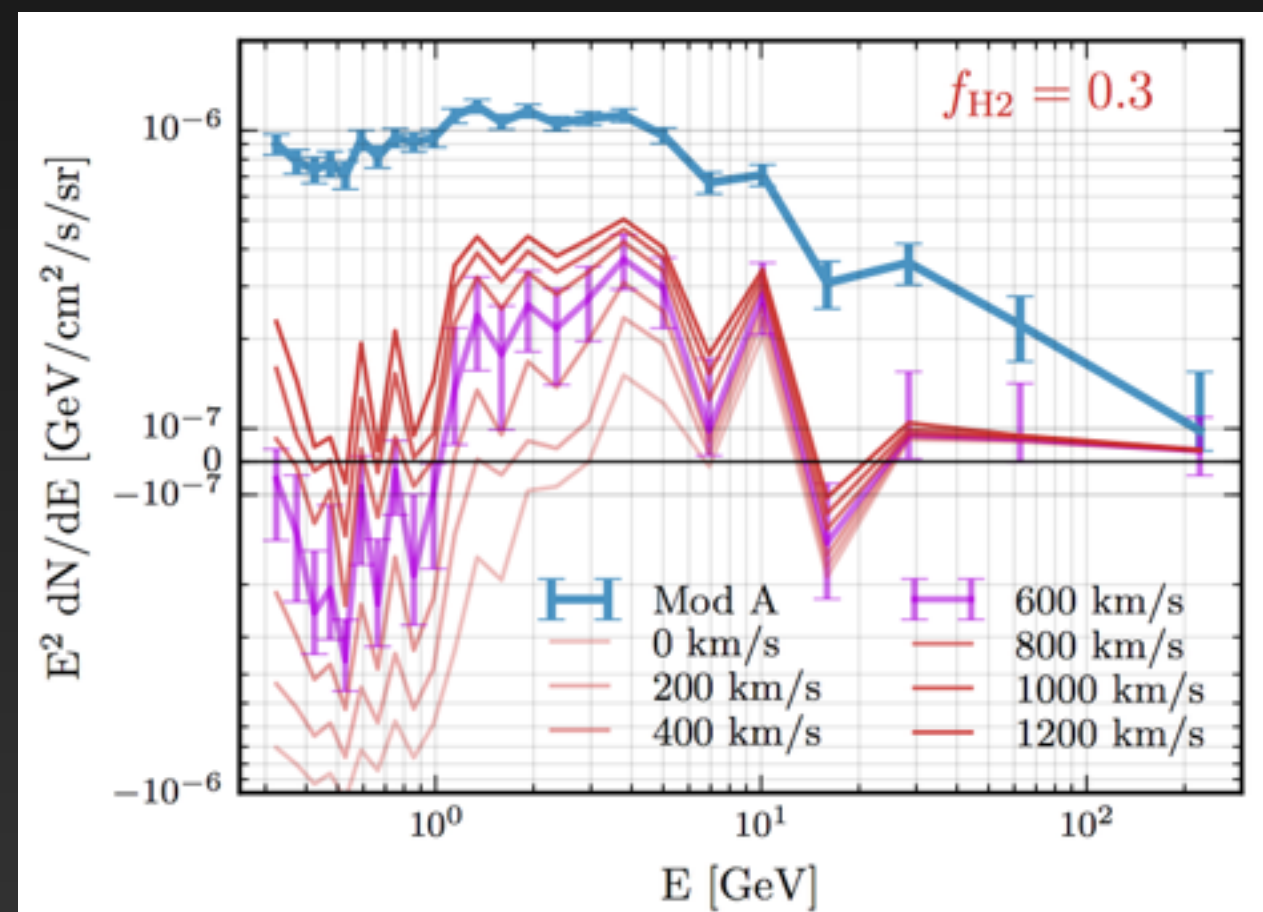
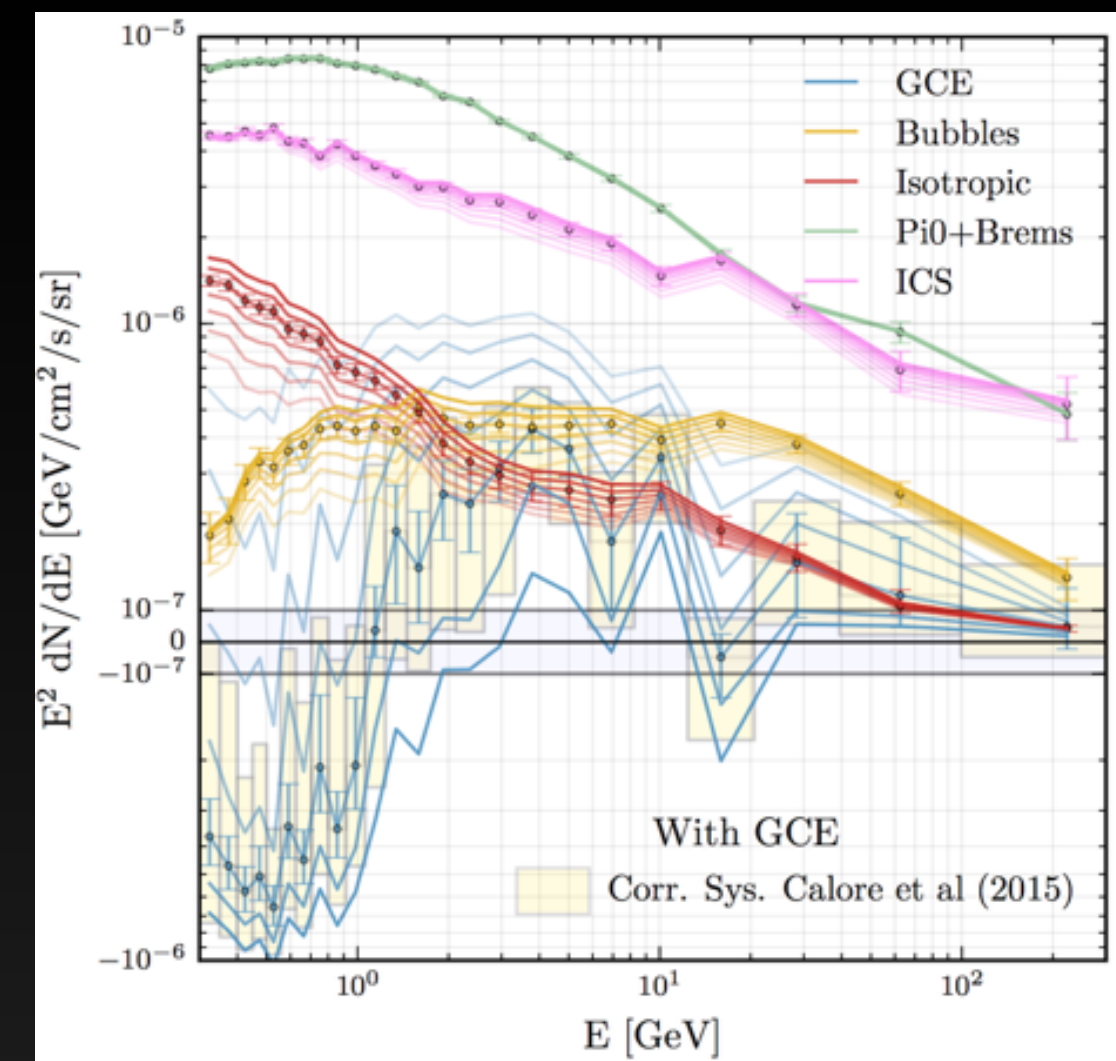
Models with a GCE component still prefer slightly lower values of f_{H_2} , but these have increased to 0.2 as well.

The Low Energy Spectrum

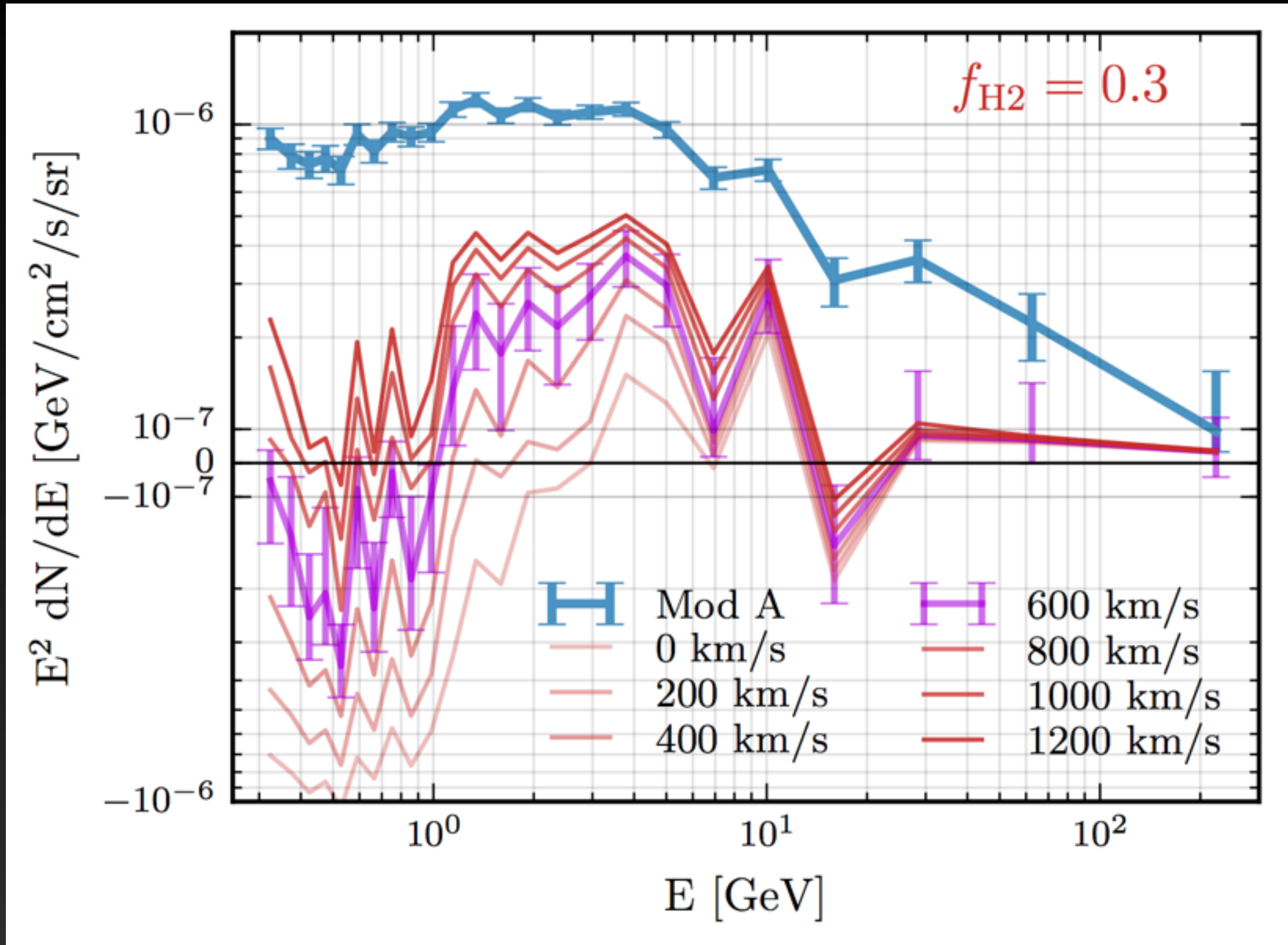
Can apply these to Galprop models by adding a new radial wind.

Advective energy losses most important for low-energy cosmic-rays, decreases the astrophysical contribution < 1 GeV.

Peak of the GeV excess returns to more than 50% of initial luminosity.

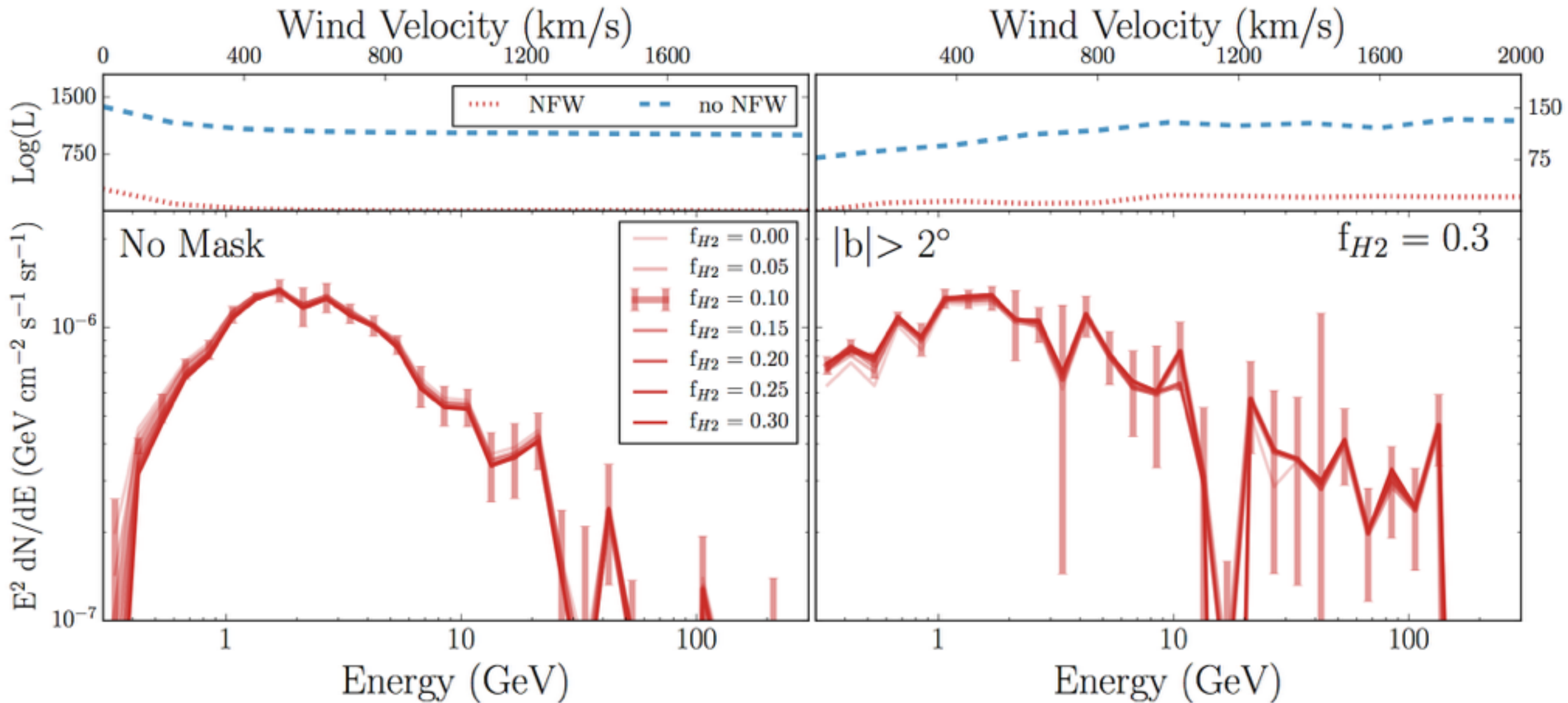


The Low Energy Spectrum



The excess lives!

The Low Energy Spectrum

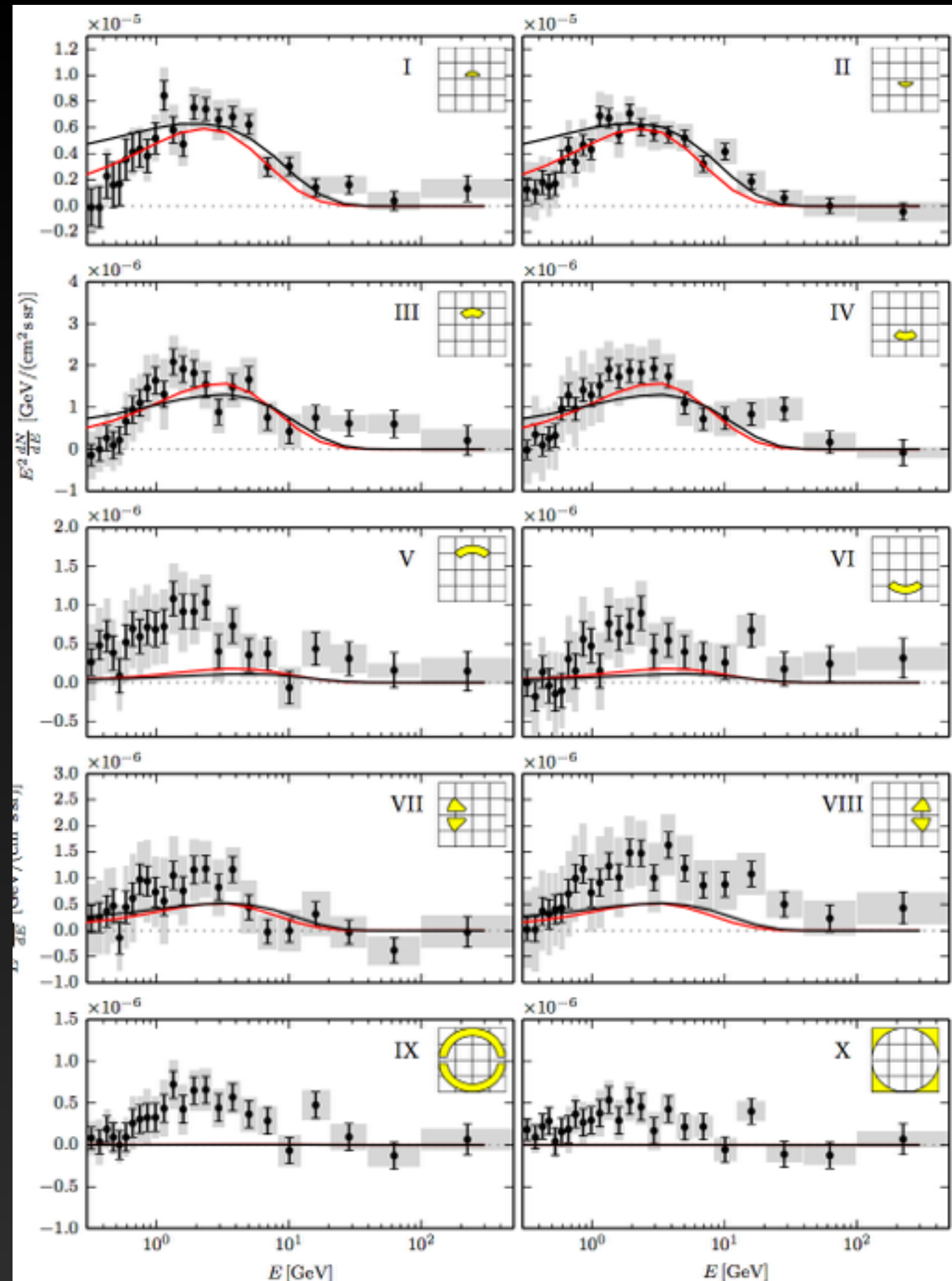


The Galactic Center models contain only a small preference for the convective winds, and the spectrum and intensity of the Galactic center excess component remains resilient.

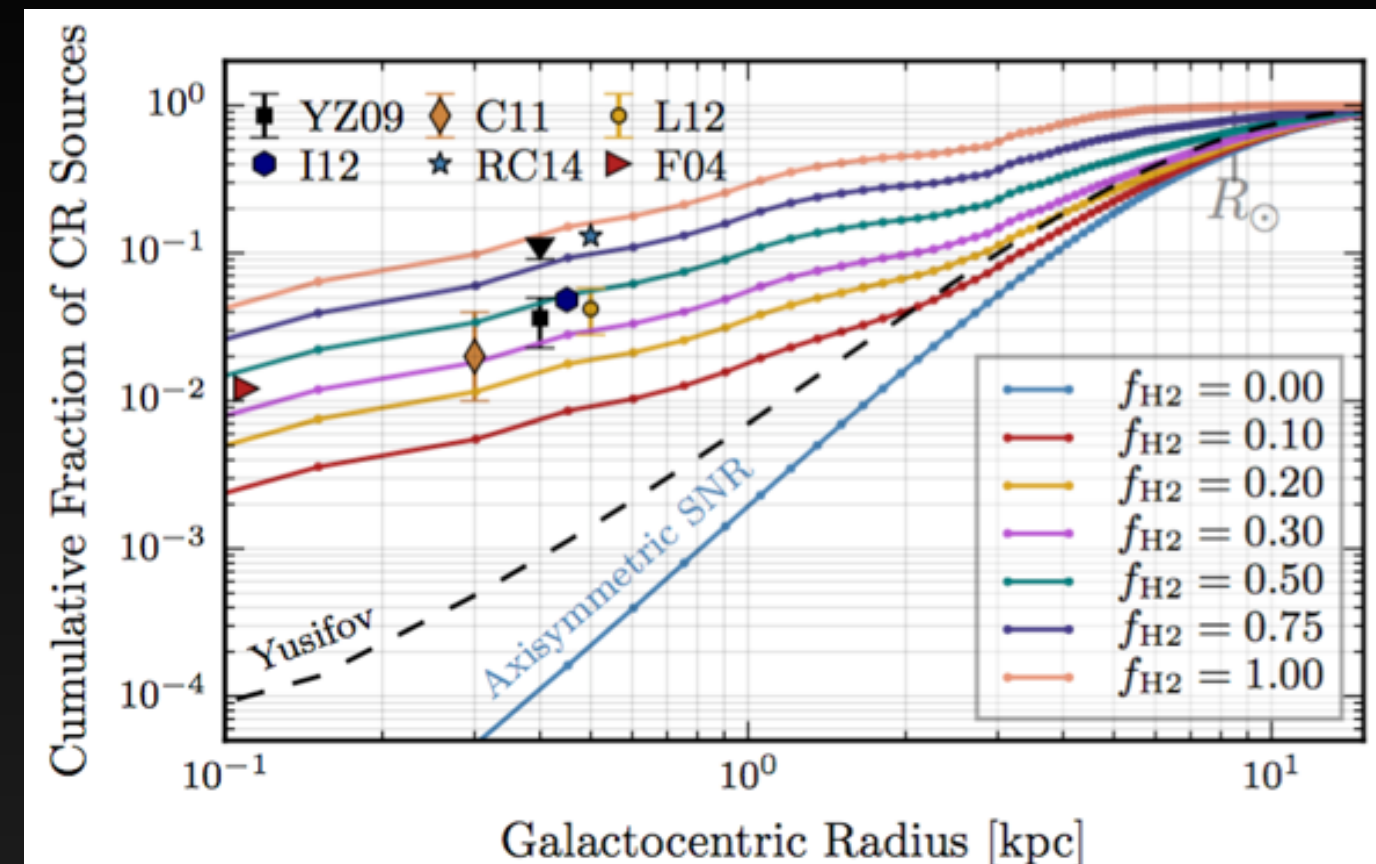
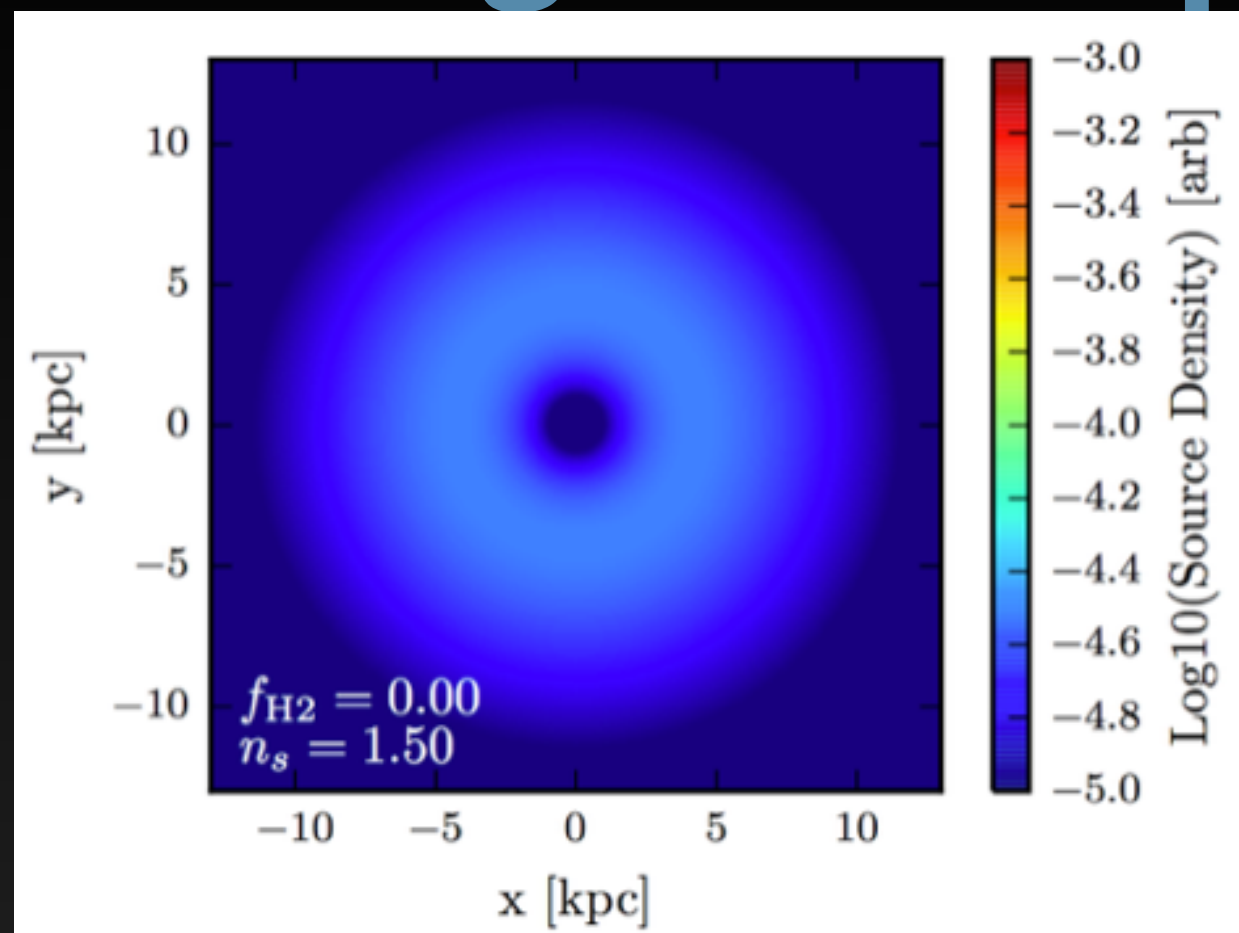
Outbursts!

So far, we have only considered steady-state diffuse emission scenarios - but the Galactic center is unlikely to be in steady state (e.g. Fermi bubbles).

An outburst of leptonic (or possibly hadronic) origin can also produce the gamma-ray excess, but only if the injected electron spectrum is extremely hard (compared to observed blazar spectra).



Waxing Philosophical....



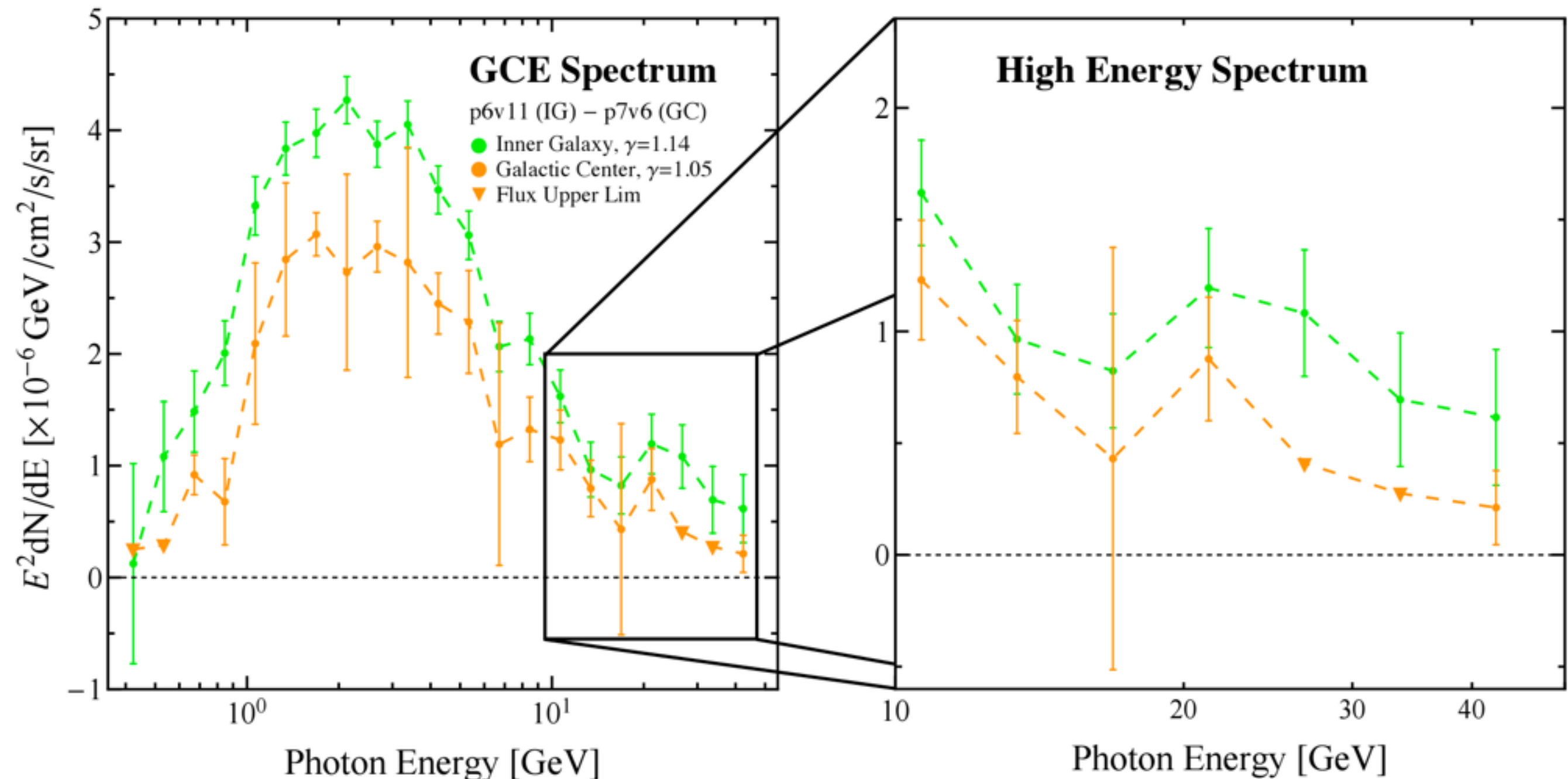
The lack of cosmic-ray injection in the GC should still be slightly disturbing. Especially when we try to answer the question: ‘excess compared to what?’

On the other hand, it seems clear that we don’t have a final answer yet. An optimal diffuse model should remove or produce an excess that is consistent among all ROIs and analysis techniques.

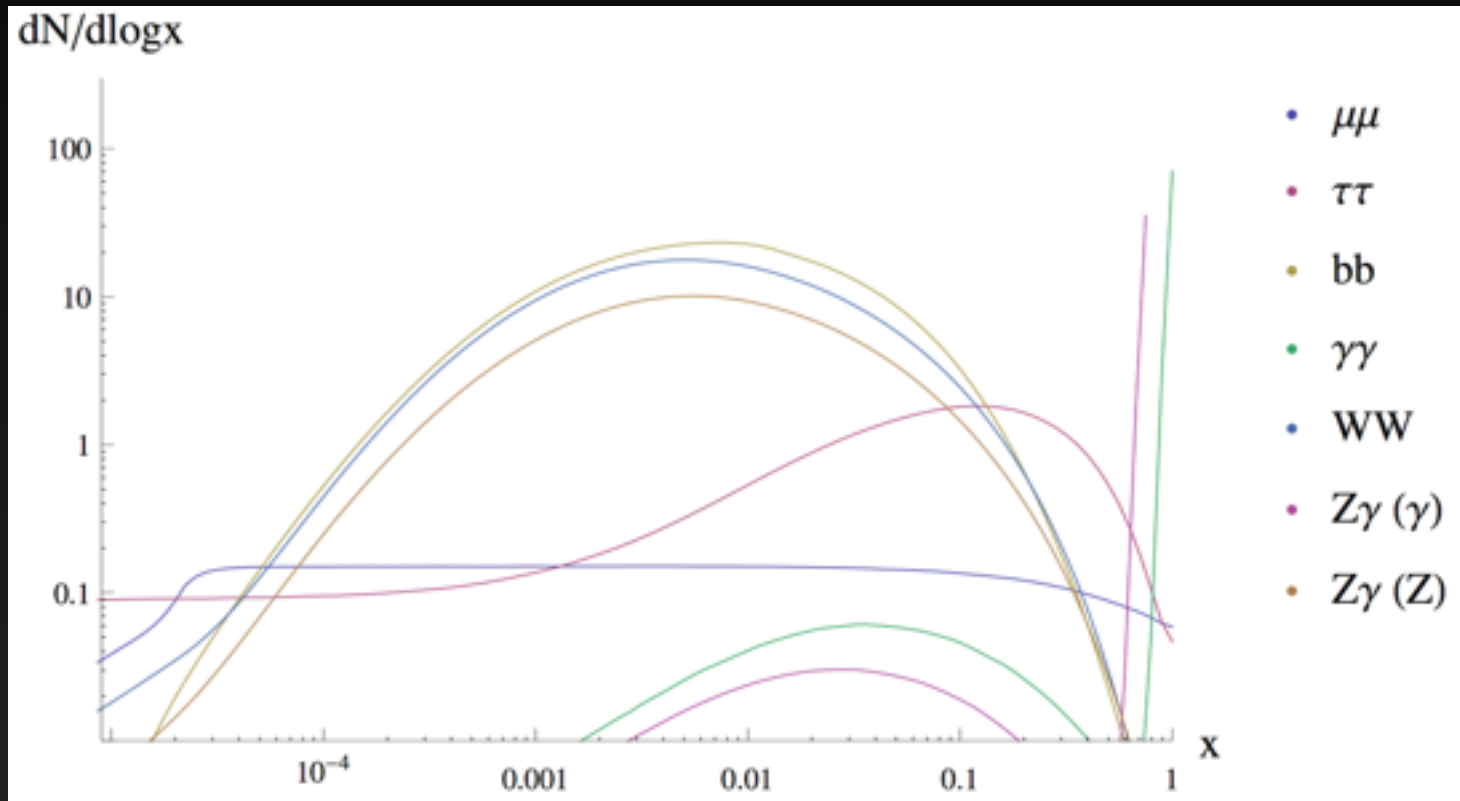
Approaching a Conclusion

- 1.) We introduce a new astrophysical emission tracer which:
 - a.) Improves the overall fit to the gamma-ray sky
 - b.) Is degenerate with properties of the gamma-ray excess
- 2.) The effect on the gamma-ray excess depends on the ROI. In signal dominated regions the NFW template produces significant emission, while in side-bands dominated regions, the excess is diminished.
- 3.) For a preferred value of $f_{\text{H}_2} \sim 0.1$, the morphology of the excess is significantly altered, producing a slightly elliptical morphology.
- 3.) This model space is not yet fully explored, new models of H₂ gas near the GC may greatly improve our fits to the gamma-ray data. There is a clear path forward with enhanced gas observations.

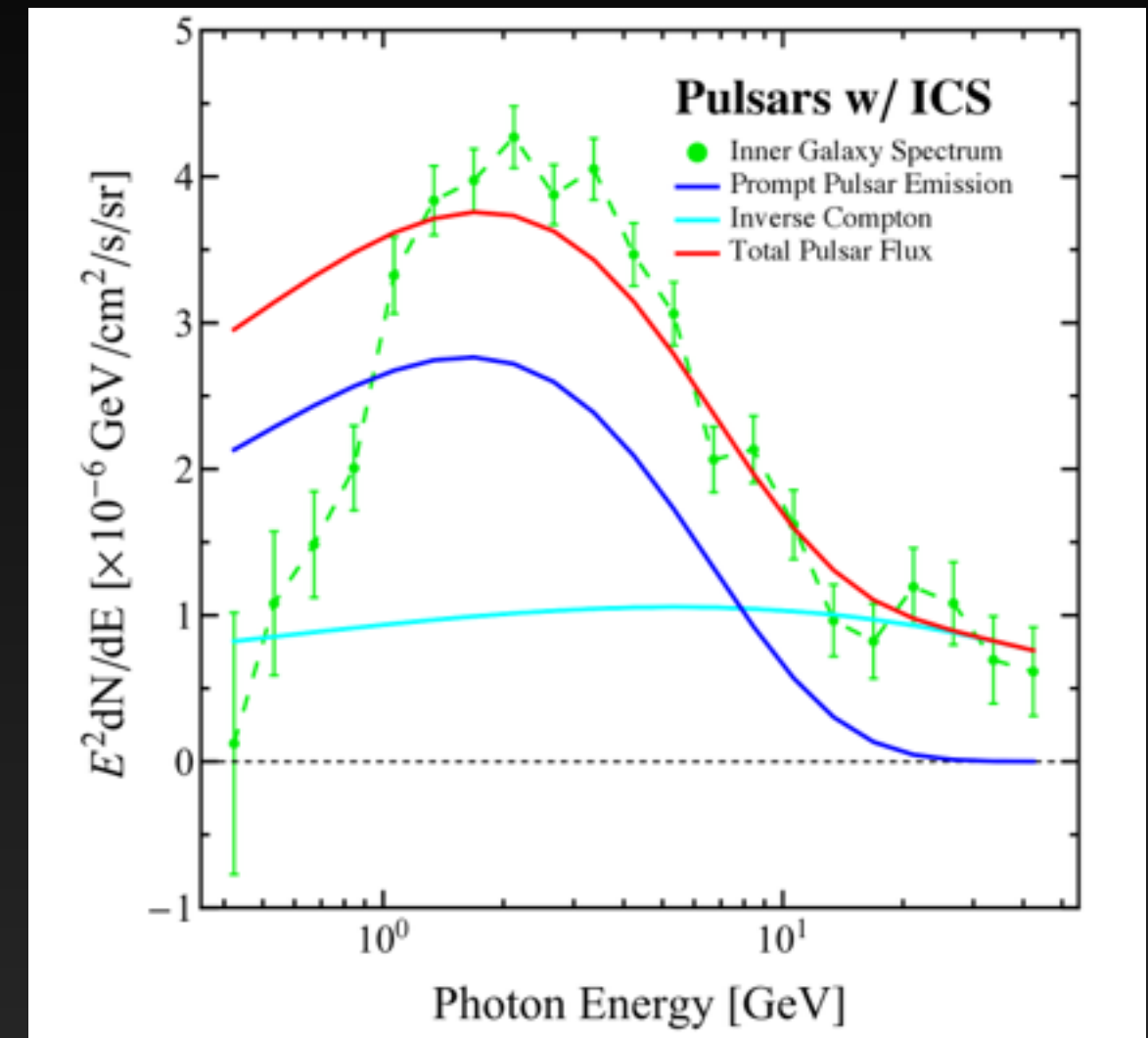
The High Energy Tail of the Gamma-Ray Excess



The High Energy Tail of the Gamma-Ray Excess



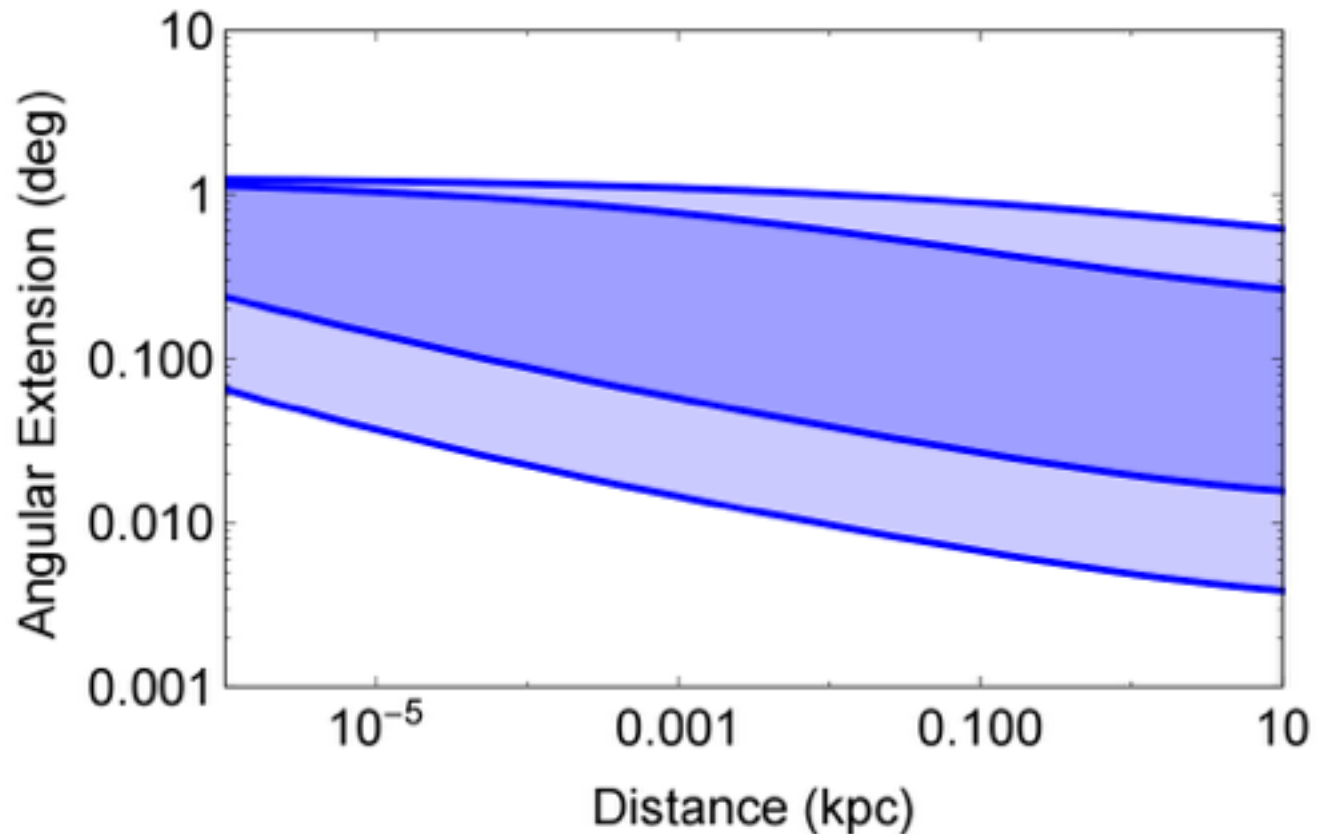
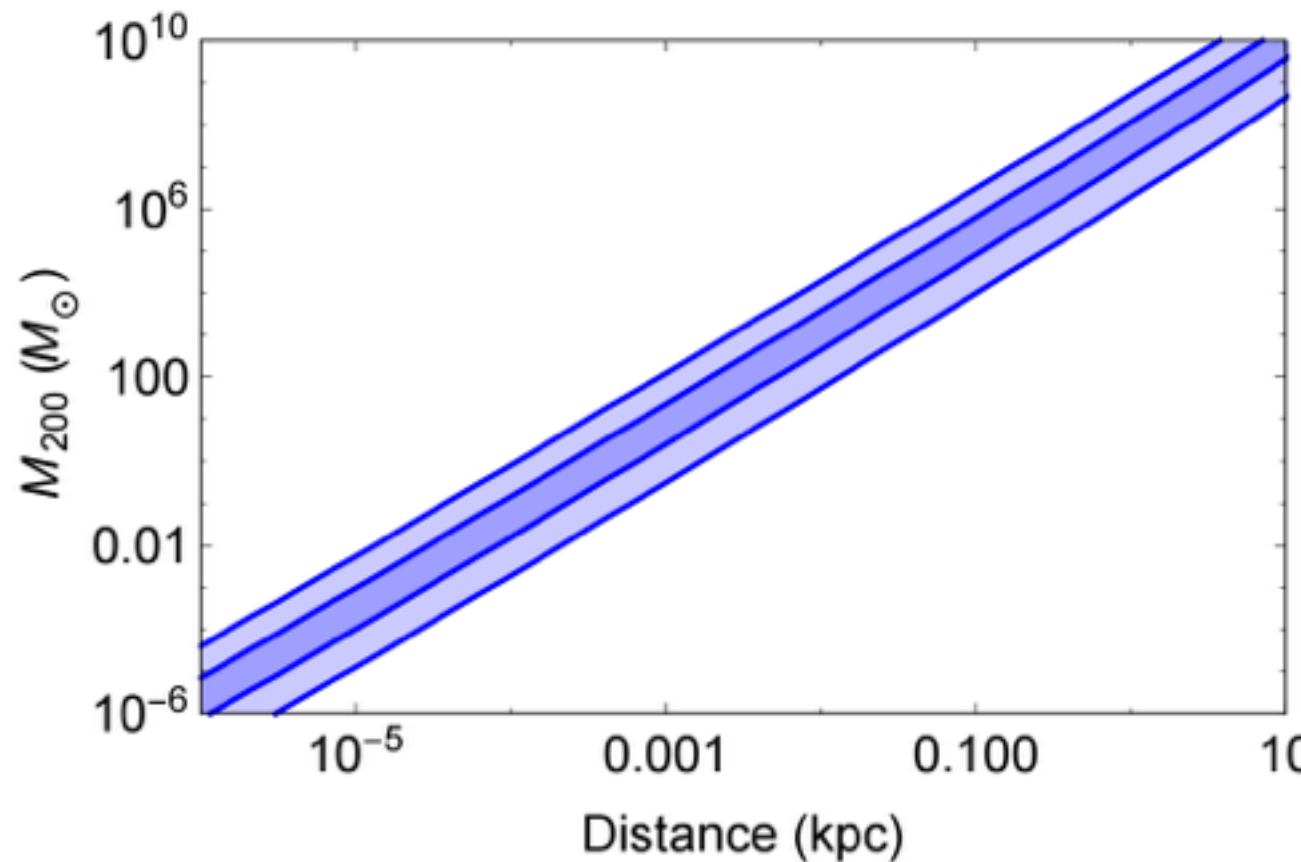
With Dark Matter



With MSPs

arXiv: 1604.01026

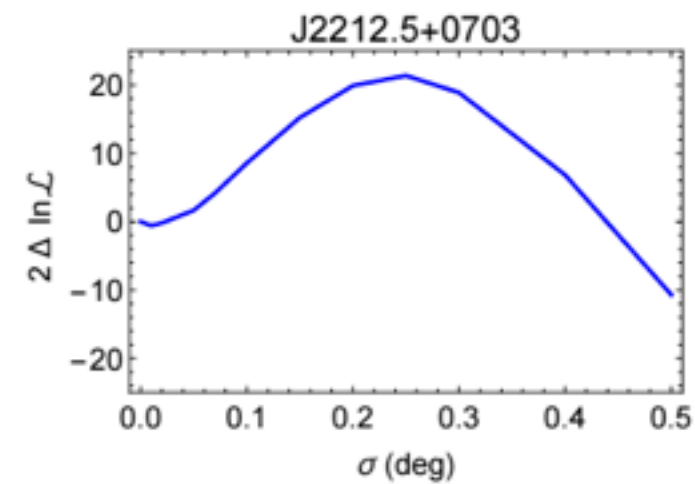
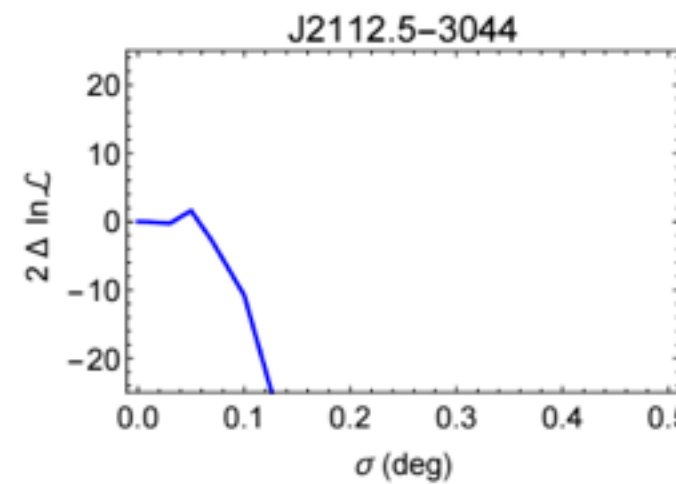
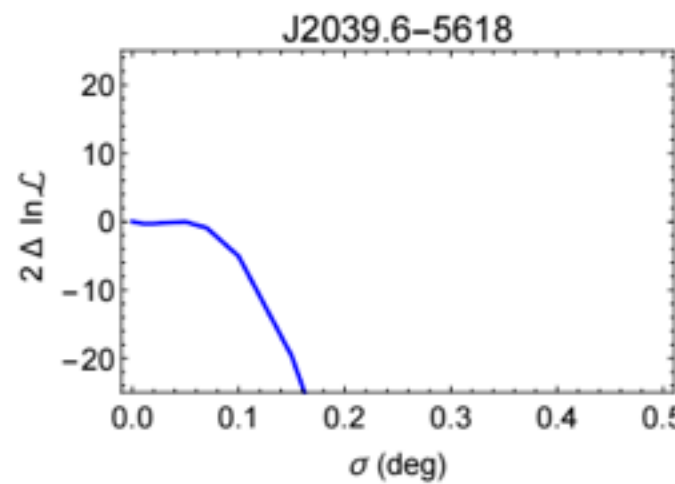
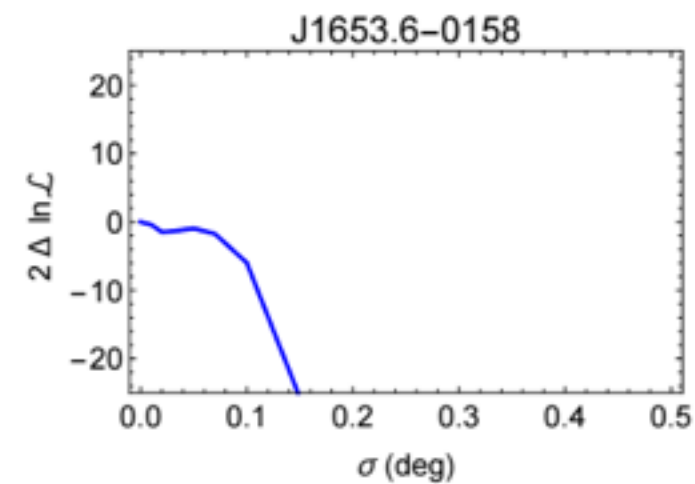
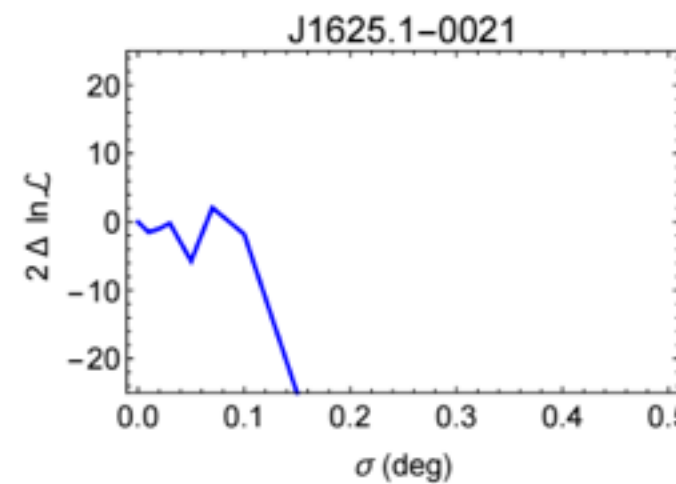
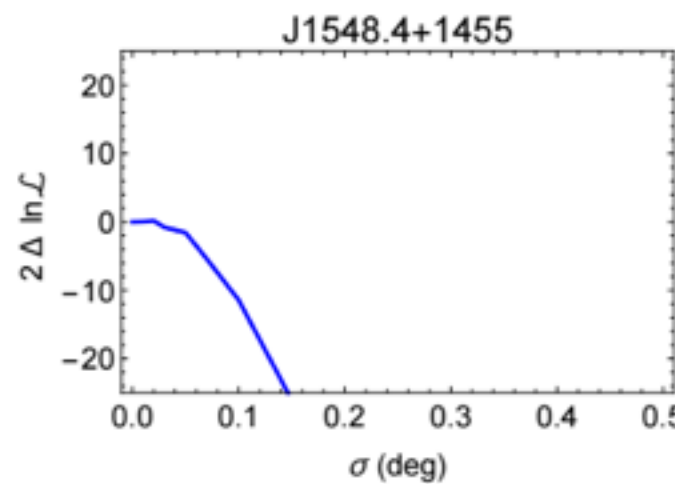
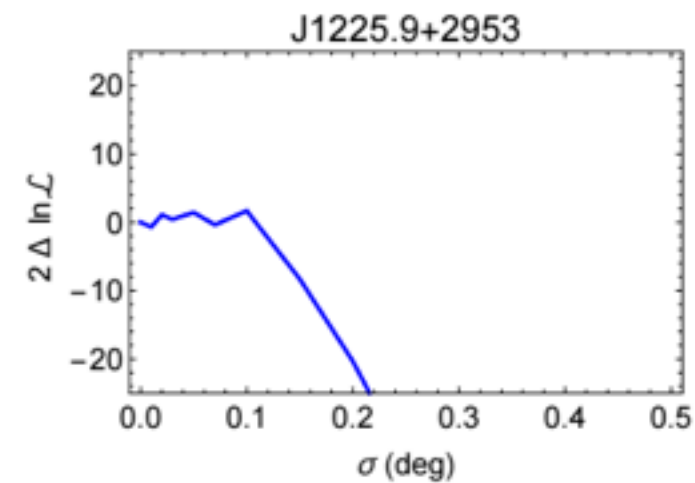
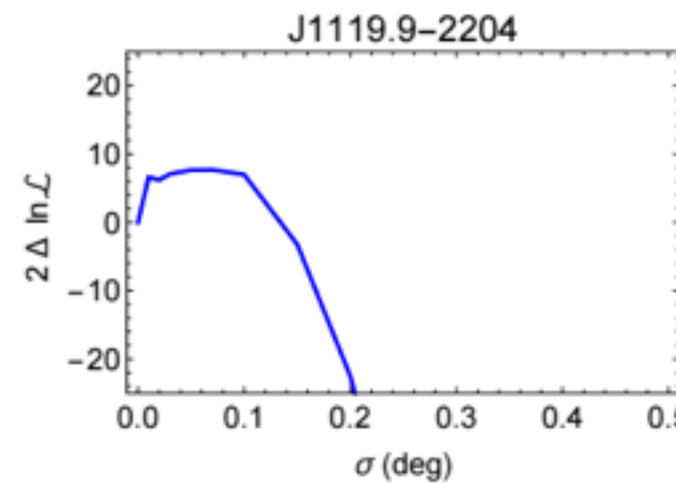
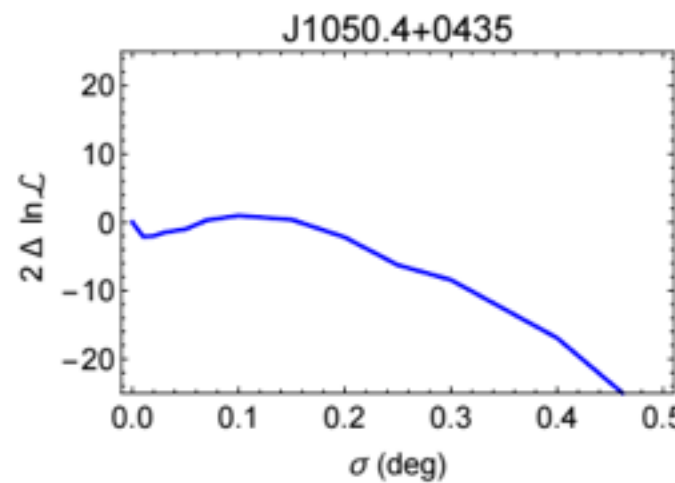
Unassociated Point Sources



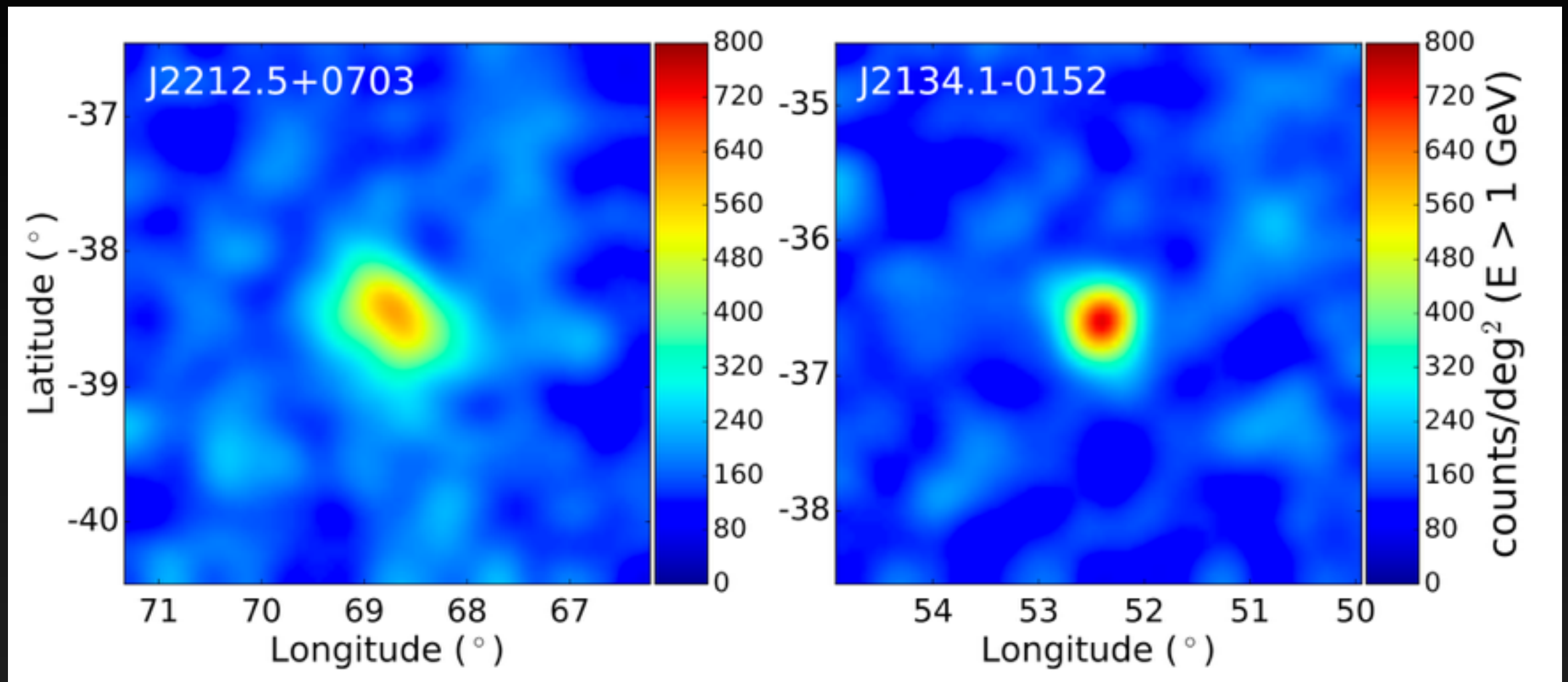
One additional smoking gun signature of dark matter annihilation would be the existence of a spatially extended, but unassociated gamma-ray source.

This could stem from dark matter subhalos of many sizes and distances.

Unassociated Point Sources



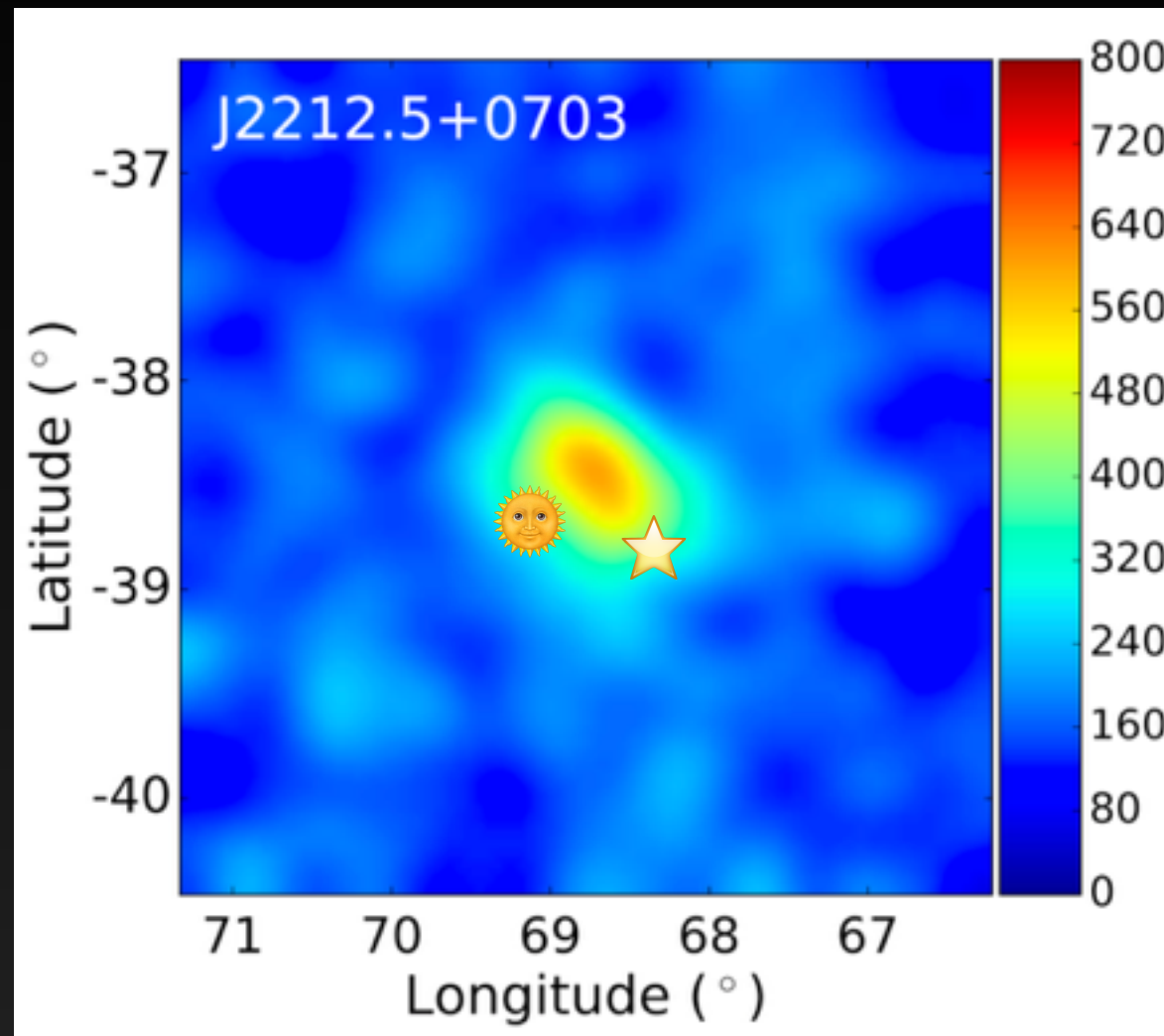
Unassociated Point Sources



The source visually appears to be spatially extended, compared to typical gamma-ray sources, and an extension that is favored at nearly 5σ .

| Source Name (3FGL) | σ | $2\Delta \ln \mathcal{L}$ |
|--------------------|---------------------------------|---------------------------|
| J2212.5+0703 | 0.25° ($< 0.31^\circ$) | 21.4 |
| J1119.9-2204 | 0.07° ($< 0.12^\circ$) | 7.7 |
| J0318.1+0252 | 0.15° ($< 0.20^\circ$) | 5.8 |
| J0953.7-1510 | 0.05° ($< 0.09^\circ$) | 2.5 |
| J1625.1-0021 | 0.07° ($< 0.10^\circ$) | 2.1 |
| J1225.9+2953 | 0.10° ($< 0.12^\circ$) | 1.7 |
| J2112.5-3044 | 0.05° ($< 0.07^\circ$) | 1.6 |
| J0523.3-2528 | $< 0.06^\circ$ | — |
| J1050.4+0435 | $< 0.21^\circ$ | — |
| J1548.4+1455 | $< 0.06^\circ$ | — |
| J1653.6-0158 | $< 0.09^\circ$ | — |
| J2039.6-5618 | $< 0.09^\circ$ | — |

Unassociated Point Sources



Unfortunately, it is currently difficult to determine whether the spatial extension results from a population of nearby point sources.

Two (of 14,467) sources are within 0.25° of the J2212 gamma-ray source.

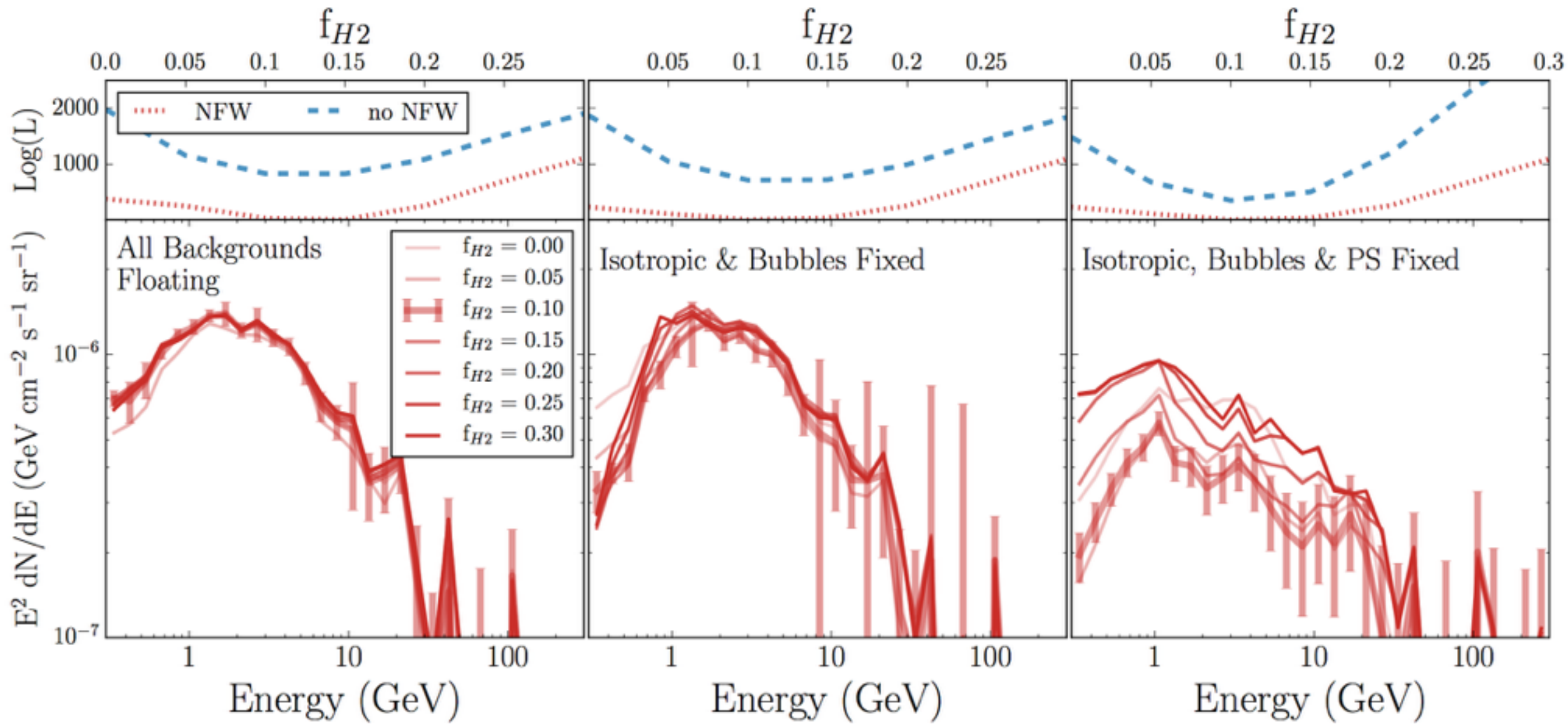
These two point sources do not themselves explain the morphology and spectrum of the source.

However, one source plus an unknown source near the center of the excess does fit.

$$\begin{aligned}\mathcal{P} &= \frac{N(N-1)}{2} \frac{\pi\alpha^2}{4\pi[1-\sin 20^{\circ}]} \\ &\approx 2.3 \times 10^{-6} \times N(N-1) \times \left(\frac{\alpha}{0.2^{\circ}}\right)^2 \\ \mathcal{P} &\approx 2.2 \times 10^{-2} \times \left(\frac{\alpha}{0.2^{\circ}}\right)^2\end{aligned}$$

Extra Slides

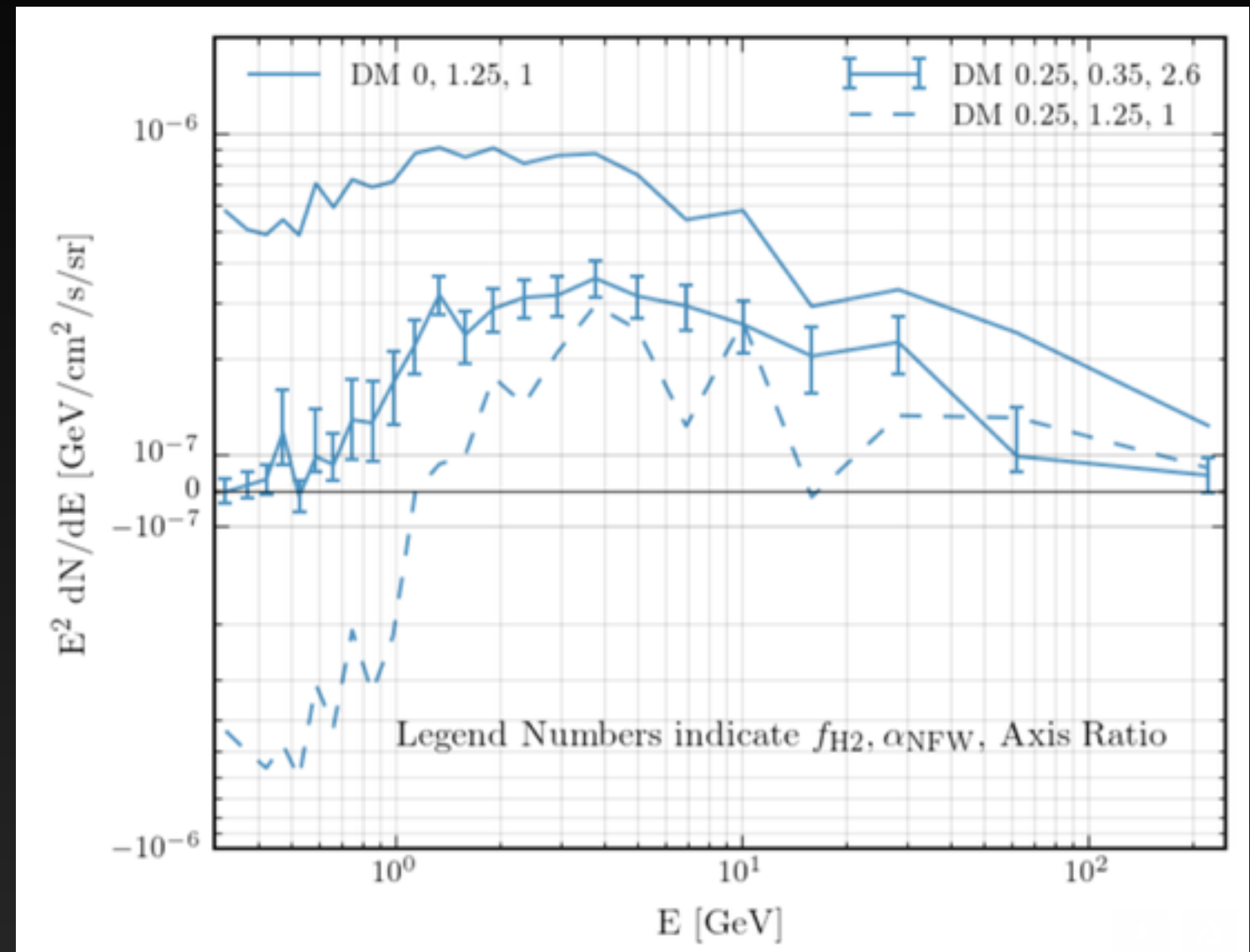
Masking 1FIG Sources in the GC



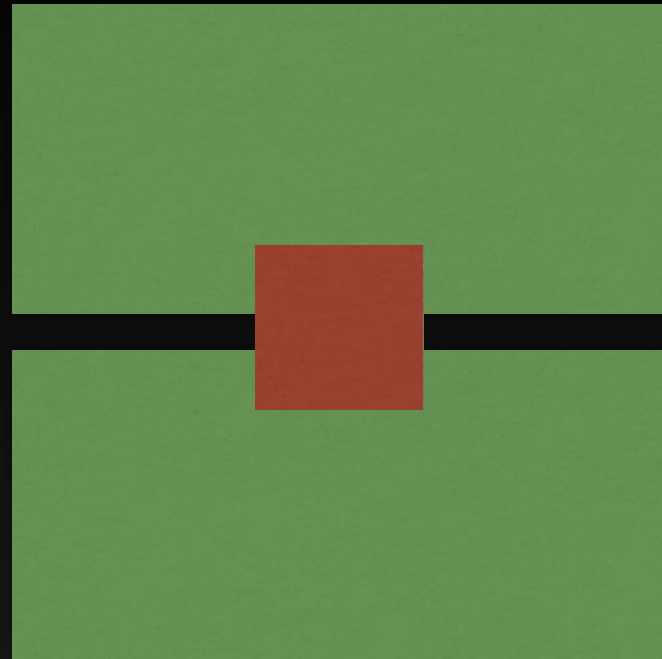
A Fermi Bubbles Component?

When the excess floats to the best fit morphological configuration, much of the excess intensity returns.

Most importantly, the over subtraction issue at low energies is fixed.



Two Analyses of the Gamma-Ray Excess



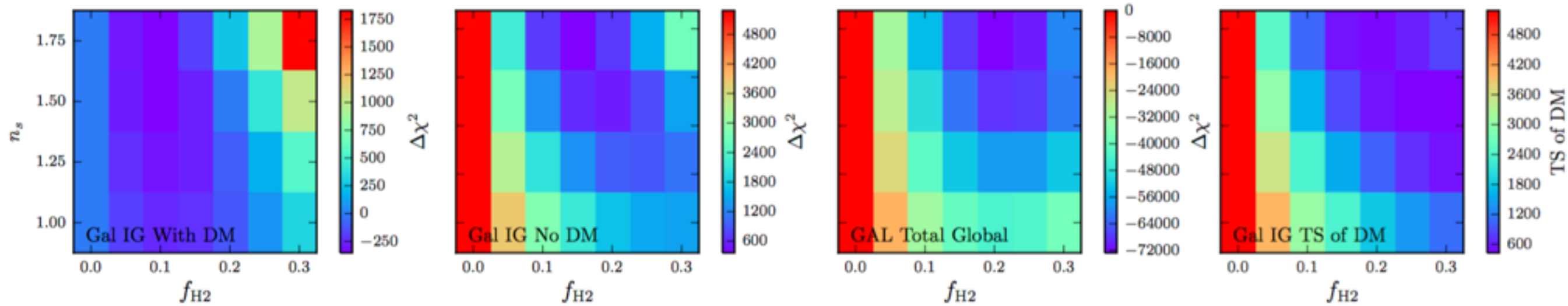
INNER GALAXY

- Mask galactic plane (e.g. $|b| > 1^\circ$), and consider $40^\circ \times 40^\circ$ box
- Bright point sources masked at 2°
- Use likelihood analysis, allowing the diffuse templates to float in each energy bin
- Background systematics controlled

GALACTIC CENTER

- Box around the GC ($10^\circ \times 10^\circ$)
- Include and model all point sources
- Use likelihood analysis to calculate the spectrum and intensity of each source
- Bright Signal

The Excess is Degenerate with $f_{\text{H}2}$



Models with no dark matter universally prefer $f_{\text{H}2} \sim 0.2$ for the $40^\circ \times 40^\circ$ region surrounding the GC.

Models with an NFW emission template prefer $f_{\text{H}2} \sim 0.1$.

The reduction in the normalization of the NFW template is ~ 1.5 for $f_{\text{H}2} \sim 0.1$, instead of a factor of 3 at $f_{\text{H}2} \sim 0.2$.

Cosmic-Ray Injection in the GC

Why Is this Done?

1.) Want to fit a simple analytic form to a profile that peaks at 4 kpc.

2.) Small datasets mean error bars near GC are large.

3.) Model of GC is unimportant for cosmic-ray propagation studies.

